

A Unified Description of the Spin–Spin and Spin–Lattice Relaxation Rates Applied to Nitroxide Spin Labels in Viscous Liquids

Bruce H. Robinson,* Annabelle W. Reese, Erin Gibbons, and Colin Mailer

University of Washington, Seattle, Washington 98195

Received: January 4, 1999

For nitroxide spin labels the application of electron and nuclear spin relaxation theory has caused a seeming paradox to develop, even in the fast motion limit. Two well-resolved EPR lines are seen when using ^{15}N nitroxide spin labels (or three lines with ^{14}N nitroxide spin labels) due to the interaction of the electron with the nitrogen nucleus. The observed line widths are related to the spin–spin relaxation rates. The different widths indicate that the spin–spin relaxation rates for the two (or three) lines depend on the nuclear manifold, or nuclear spin state z quantum number. The theory (developed by Kivelson and Freed) treated each line independently and gave a quantitative accounting of the differences seen in the relaxation rates of the lines. When the same treatment is applied to the spin–lattice relaxation rates, a strong dependence of the spin–lattice relaxation rate on the particular line (nuclear manifold) chosen is predicted. However, the experimental spin–lattice relaxation rates show no dependence on the nuclear manifold (nuclear quantum number). The treatment presented here shows that by following the operator method of Abragam one can develop a consistent picture for both spin–lattice relaxation and spin–spin relaxation that leads to theoretical predictions that agree with the experimental results.

Introduction

Nitroxide spin labels have been used as probes of molecular motion in the biological and physical sciences for the past 25 years.¹ Electron paramagnetic resonance (EPR), in conjunction with the spin-label methodology, is a very powerful technique for studying molecular dynamics over a range from picoseconds to milliseconds in rotational correlation times. One utilizes indirect information, such as spin–lattice relaxation rates, $R_{1e} = T_{1e}^{-1}$, or motionally induced changes in spectral widths, i.e., the spin–spin relaxation rate, $R_{2e} = T_{2e}^{-1}$, to make a statement about the dynamics of the system of interest. Continuous wave (CW)-EPR, using spectral line widths and slow-motion theory, gives information on motion on the pico- to nanosecond time scale. CW-saturation transfer (ST)-EPR¹ produces a spectrum whose shape is determined by a competition among relaxation rates, magnetic field modulation rate, and the motional rates in the microsecond to millisecond regime. Application of line-shape simulation methods to aid data analysis has been limited to relatively simple dynamical models since truly accurate simulations require detailed knowledge of all relaxation processes. Given the ubiquity of EPR spin label usage in liquids, it is somewhat surprising that a clear understanding of longitudinal relaxation mechanisms has not emerged until now.

The purpose of this paper is to resolve a difference between theory and experiment in the spin–lattice relaxation of nitroxide spin labels in liquids. The experimental spin–spin relaxation rate, R_{2e} , and the spin–lattice relaxation rate, R_{1e} , have different dependencies upon the nitrogen nuclear spin quantum number m : R_{2e} has a strong dependence on m , while R_{1e} has no such dependence. Theory for R_{2e} , based on the electron nuclear dipolar interaction (END), has been extensively developed by Kivelson² and Freed.³ This theory is reasonably complete and has been verified in many experiments.^{3–6}

The most widely used form of the theory for R_{2e} states that the apparent line width $R_{2e}(m)$ is given by

$$R_{2e}(m) = A + Bm + Cm^2 \quad (1)$$

where m is the (z component) nuclear quantum number for nitrogen, and A , B , and C are m -independent quantities.³ For ^{15}N $m = -1/2$ or $1/2$ and for ^{14}N $m = -1, 0$, or 1 . The Kivelson theory for the spin–lattice relaxation rate R_{1e} predicts a similar m dependence for the electron nuclear dipolar (END) contribution. Specific application of the Kivelson theory to spin label relaxation was first done by Percival and Hyde (eq 2 of ref 7) with the result

$$R_{1e}^{\text{END}}(m) = (0.39 - 1.91m + 2.89m^2) \frac{\tau_c}{1 + \epsilon \omega_o^2 \tau_c^2} \times 10^{16} \text{ s}^{-1} \quad (2)$$

where τ_c is the rotational correlation time, ω_o is the spectrometer frequency, and ϵ is a constant of order unity.³ The m coefficients are calculated from the g and A values for the TANOL label (4-hydroxy-2,2,6,6-tetramethylpiperidine- ^{14}N -1-oxyl)⁷ using eq A-8 in the Appendix.

Another mechanism considered by Percival and Hyde to be important in spin label relaxation is that of spin rotation (SR),^{7,8} an m independent process with rate given by

$$R_{1e}^{\text{SR}} = \sum_{i=x,y,z} (g_{ii} - 2.0023)^2 / 9\tau_c \quad \text{s}^{-1} \quad (3A)$$

where the g_{ii} are the three g values of the nitroxide spin label. Percival and Hyde showed that the relaxation rates predicted by END+SR theory did not agree with experiment.

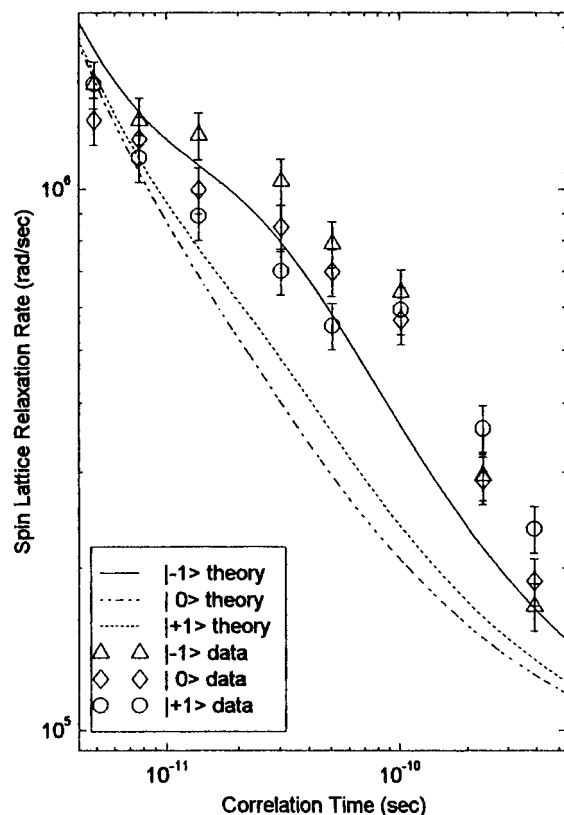


Figure 1. Plot of spin–lattice relaxation theory and experiment of an ^{14}N nitroxide spin label in a liquid. The experimental spin–lattice relaxation data of Percival and Hyde⁷ for TANOL in *sec*-butylbenzene (SBB) are shown as open triangles, diamonds, and circles for nuclear spin quantum numbers $m = -1, 0$, and $+1$, respectively. The errors are those reported on the basis of reproducibility of experiments.⁷ The correlation times τ_c for the samples were recalculated by us⁵ from the SBB viscosity data given in ref 7. The solid, dotted, and dashed lines are the spin–lattice relaxation rates predicted from the sum of eqs 2 and 3 in the text for $m = -1, 0$, and 1 , respectively. The theory was fit using the **A** and **G** tensors⁷ and the spin diffusion parameters⁷ given elsewhere. No parameters were adjusted in fitting the theory to the data.

Our relaxation studies of spin labels⁹ concluded that a generalized spin diffusion (SD) mechanism had also to be added. This predicts that the spin diffusion relaxation rate, R_{1e}^{SD} , is

$$R_{1e}^{\text{SD}} = 0.13 \times 10^6 \left(\frac{2\omega_o\tau_c}{1 + (\omega_o\tau_c)^2} \right)^{1/4} \text{ s}^{-1} \quad (3B)$$

where τ_c and ω_o are the rotational correlation time and the spectrometer frequency, respectively.

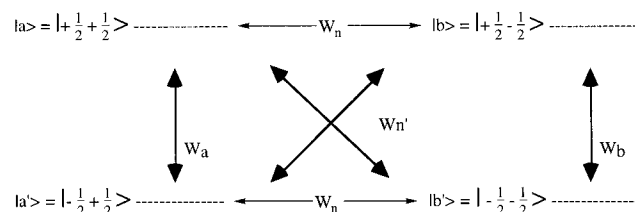
We show in Figure 1 a plot of the experimental spin–lattice relaxation rates of Percival and Hyde⁷ for the $m = -1, 0$, and $+1$ lines of an ^{14}N spin label, along with the m dependent rates calculated from the sum of eqs 2 and 3. The data are in reasonable agreement with the relaxation rates corresponding to the $m = -1$ case (solid line). As can be seen from the dashed and dotted lines, the $m = 0$ and $+1$ cases predict relaxation rates about a factor of 3 smaller than for the $m = -1$ case. Clearly, the experimental data do not agree, e.g., the rate data for the $m = 0$ case (diamonds) should always be less than the other two data sets but in fact lie both higher and lower than them. The error bars on the data are those estimated from the experiments: the predicted differences between m values would easily be seen in the data if the m dependence of the END mechanism were correct. We recently measured the relaxation

rates of both ^{14}N and ^{15}N spin labels using pulsed electron–electron double resonance over a much wider correlation time range (picoseconds to milliseconds) than that of Percival and Hyde and also observed no m dependence.⁹ These discrepancies between the existing theory and the results of experiments in two different laboratories forced us to re-examine the theory. This paper aims to explain the line independence of the R_{1e} process, while retaining the experimentally confirmed m dependence of R_{2e} given by eq 1.

Theory

There are two different theoretical treatments for the development of relaxation expressions. The first is the Redfield method,¹⁰ which examines elements of a density matrix, χ . The second is Abragam's, which develops the relaxation of coupled observables.¹¹ Both are very closely related, and if one were to do a full calculation with either method, one would of course obtain the same result. A complete interpretation of an observable requires that a sum be made over all the elements of the density matrix, as is done in Abragam's treatment. Redfield theory, however, allows for a restricted sum over just the electronic indices to obtain m -dependent "pseudo-observables". It is this limited summation in Redfield theory, and an approximate treatment of the couplings to other density matrix elements, that lead to the prediction of a strong m dependence of R_{1e} . In the next section we develop a unified theory for both the R_{2e} and the R_{1e} relaxation rates, extending the approach taken by Abragam. We will demonstrate, using Abragam's approach, that such a unified treatment is capable of solving two confusing issues: (1) How is it possible that manifold *independent* relaxation rates lead to manifold *dependent* line widths? (2) How is it possible for spin–spin relaxation to be manifold *dependent* and the spin–lattice relaxation to be manifold *independent*? The theory is applied to CW-EPR line shapes and to the spin–lattice relaxation times seen in pulsed saturation recovery and pulsed ELDOR experiments.

Density Matrix Elements and Observables. The theory begins with the well-established density matrix form for the evolution of the spin system. Before proceeding further it is useful to show how the standard Solomon equations for relaxation¹² can be connected with Abragam's observable relaxation picture. For a simple $S = 1/2, I = 1/2$ spin system we have the four level energy level diagram:¹³



W_a and W_b are the spin–lattice relaxation rates of lines a and b , W_n is the nuclear spin–lattice relaxation rate, and W_n' is the cross relaxation rate (p 95 of ref 14). We define $W_e = (W_a + W_b)/2$. The diagonal density matrix elements corresponding to the level population differences are $\chi_a = \langle a|\chi|a\rangle = \rho_{aa} - \rho_{aa}^o$ etc., where ρ is the density matrix and ρ^o is the density matrix at equilibrium. The rate equation for χ_a is:

$$\partial\chi_a/\partial t = -W_a(\chi_a - \chi_{a'}) - W_n(\chi_a - \chi_b) - W_n'(\chi_a - \chi_{b'})$$

The full rate equation for all four elements is, in matrix form,

$$\begin{pmatrix} \dot{\chi}_a \\ \dot{\chi}_{a'} \\ \dot{\chi}_b \\ \dot{\chi}_{b'} \end{pmatrix} = - \begin{bmatrix} W_a + W_n + W'_n & -W_a & -W_n & -W'_n \\ -W_a & W_a + W_n + W'_n & -W'_n & -W_n \\ -W_n & -W'_n & W_b + W_n + W'_n & -W_b \\ -W'_n & -W_n & -W_b & W_b + W_n + W'_n \end{bmatrix} \begin{pmatrix} \chi_a \\ \chi_{a'} \\ \chi_b \\ \chi_{b'} \end{pmatrix}$$

Defining the ratios (following Freed¹⁴) as $b = W_n/W_e$, $b' = W'_n/W_e$, and $b_x = (W_a - W_b)/2W_e$ leads to the following equation:

$$\begin{pmatrix} \dot{\chi}_a \\ \dot{\chi}_{a'} \\ \dot{\chi}_b \\ \dot{\chi}_{b'} \end{pmatrix} = -W_e \times \begin{bmatrix} 1 + b_x + b + b' & -1 - b_x & -b & -b' \\ -1 - b_x & 1 + b_x + b + b' & -b' & -b \\ -b & -b' & 1 - b_x + b + b' & -1 + b_x \\ -b' & -b & -1 + b_x & 1 - b_x + b + b' \end{bmatrix} \begin{pmatrix} \chi_a \\ \chi_{a'} \\ \chi_b \\ \chi_{b'} \end{pmatrix}$$

These density matrix elements are related to the quantum mechanical observables of the magnetization, but not all of these “observables” are necessarily detectable experimentally. The quantum mechanical observables corresponding to this set of diagonal density matrix elements, which are linear combinations of the χ 's, are

$$\langle 1/2 \rangle = \frac{1}{2} \text{tr}\{\chi\} = \frac{1}{2}[\chi_a + \chi_{a'} + \chi_b + \chi_{b'}]$$

$$\langle I_o \rangle = \text{tr}\{I_o \chi\} = \frac{1}{2}[(\chi_a + \chi_{a'}) - (\chi_b + \chi_{b'})]$$

$$\langle S_o \rangle = \text{tr}\{S_o \chi\} = \frac{1}{2}[(\chi_a - \chi_{a'}) + (\chi_b - \chi_{b'})]$$

$$\langle 2S_o I_o \rangle = \text{tr}\{2S_o I_o \chi\} = \frac{1}{2}[(\chi_a - \chi_{a'}) - (\chi_b - \chi_{b'})]$$

Writing these in matrix form we find the relation between the observables and the diagonal elements of the density matrix:

$$\begin{pmatrix} \langle 1/2 \rangle \\ \langle I_o \rangle \\ \langle S_o \rangle \\ \langle 2I_o S_o \rangle \end{pmatrix} = \frac{1}{2} \begin{bmatrix} 1 & 1 & 1 & 1 \\ 1 & 1 & -1 & -1 \\ 1 & -1 & 1 & -1 \\ 1 & -1 & -1 & 1 \end{bmatrix} \begin{pmatrix} \chi_a \\ \chi_{a'} \\ \chi_b \\ \chi_{b'} \end{pmatrix}$$

Substituting for the χ in the differential equation above, we get the differential equation for the observables:

$$\begin{pmatrix} \dot{\langle 1/2 \rangle} \\ \dot{\langle I_o \rangle} \\ \dot{\langle S_o \rangle} \\ \dot{\langle 2I_o S_o \rangle} \end{pmatrix} = -2W_e \begin{bmatrix} 0 & 0 & 0 & 0 \\ 0 & b + b' & 0 & 0 \\ 0 & 0 & 1 + b' & b_x \\ 0 & 0 & b_x & 1 + b \end{bmatrix} \begin{pmatrix} \langle 1/2 \rangle \\ \langle I_o \rangle \\ \langle S_o \rangle \\ \langle 2I_o S_o \rangle \end{pmatrix} - \begin{bmatrix} 0 & 0 & 0 & 0 \\ 0 & R_{1n} & 0 & 0 \\ 0 & 0 & R_{1e} & R_{1x} \\ 0 & 0 & R_{1x} & R'_{1e} \end{bmatrix} \begin{pmatrix} \langle 1/2 \rangle \\ \langle I_o \rangle \\ \langle S_o \rangle \\ \langle 2I_o S_o \rangle \end{pmatrix} \quad (4)$$

where $S_o \equiv S_z$ and $I_o \equiv I_z$ and $2S_o I_o \equiv 2S_z I_z$. The structure of the relaxation matrix, when seen in terms of observables (eq 4) is greatly simplified and is diagonal except for the b_x term. R_{1n} , R_{1e} , R'_{1e} , and R_{1x} are defined in terms b , b' , and W_e in eq 4:

$$2W_e \begin{pmatrix} b + b' \\ 1 + b' \\ 1 + b \end{pmatrix} \equiv \begin{pmatrix} R_{1n} \\ R_{1e} \\ R'_{1e} \end{pmatrix}$$

and correspond to the notation of Abragam (Chapter 8¹¹). To further connect the theory of observables to the Solomon relaxation diagram, we can obtain expressions for b and b' in terms of R_{1n} , R_{1e} , and R'_{1e} . Solving for b , b' , and W_e , yields

$$\begin{aligned} 2W_e &= \frac{R_{1e} + R'_{1e} - R_{1n}}{2} \\ b &= \frac{R'_{1e}}{2W_e} - 1 = \frac{R_{1n} + R'_{1e} - R_{1e}}{4W_e} \\ b' &= \frac{R_{1e}}{2W_e} - 1 = \frac{R_{1e} + R_{1n} - R'_{1e}}{4W_e} \end{aligned} \quad (5)$$

We can identify two important observables with populations of the longitudinal components:¹³ the observable $\langle I_o \rangle$ arises naturally out of the Solomon-type population diagram but is usually neglected in population analyses because the coupling to electron observables is usually small. R_{1n} , R_{1e} , and R'_{1e} represent relaxation of each of the observables, as though they were independent. Inspection of eq 4 shows that the electron Z magnetization, $\langle S_o \rangle$ relaxes at a rate $R_{1e} = 2W_e(1 + b') = 2W_e + 2W'_n$, which is not simply $2W_e$. Similarly, $\langle 2S_o I_o \rangle$ relaxes at rate $2W_e(1 + b) = 2W_e + 2W_n$. This agrees in form with Yin and Hyde's treatment¹³ except that W'_n arises here from mechanisms *other* than bimolecular collision exchange. Moreover, each relaxation rate can be due to several processes¹⁴ occurring simultaneously. Population analysis, viewed in terms of the relaxation of observables, results in diagonal matrix elements for each component of magnetization, i.e., direct relaxation processes.

Redfield Theory and Abragam Formulation. There is literature precedent for having relaxation rates not depend upon nuclear quantum number. Abragam¹¹ has developed relaxation processes in a way that is independent of nuclear quantum number, m , and independent of the choice of basis set. He gives a clear definition to the relaxation of a particular observable component of the magnetization, e.g., $\langle S_x \rangle$, $\langle S_y \rangle$ for the electron, and $\langle I_x \rangle$, $\langle I_y \rangle$ for the nitrogen nucleus upon which our theory is built. Relaxation is considered to take place using only the well-known, and understood, electron nuclear dipolar (END) and chemical shift anisotropy (CSA) mechanisms. The Hamiltonian consists of the CSA for the electron, the END interaction of the electron and the nitrogen nucleus, and a time dependent radio frequency term (see the Appendix for details of all the operators). It is easy to add the additional mechanisms given in eq 3 if desired, but for simplicity, we neglect it in this treatment. The required stochastic process is assumed to be isotropic Brownian motion. In the fast motion regime where rotational correlation times are shorter than about 10 ns, only orientation independent terms need to be retained in the zeroth-order Hamiltonian:

$$H = \omega_o S_o + \omega_n I_o + \bar{a} \sum_{p=-1}^1 (-1)^p S_p I_{-p} + \epsilon(t)$$

$$\text{where } \epsilon(t) = h \sum_{p=-1}^1 p S_p \left(\frac{(-1)^p}{\sqrt{2}} e^{ip(\omega t + \phi)} \right) \quad (6)$$

S_p and I_p are the spin operators for the two particles: the S spin represents the electron and the I spin represents the nitrogen nucleus for a spin label. For simplicity we will assume the nitrogen nucleus is ^{15}N with $m = \pm 1/2$. The Larmor frequency is $\gamma_e H_o = \omega_o$, and the radio frequency (rf) driving term, $\epsilon(t)$, affects only the S spins, because $\gamma_n H_o$, the resonance frequency of the nuclear I spin, is much less than the rf driving frequency, ($\gamma_n \approx 10^{-3} \gamma_e$). The relation of the tensor operators to the Cartesian operators and the definition of the p index are

$$S_{\pm 1} = \frac{\mp 1}{\sqrt{2}} (S_x \pm i S_y); \quad S_o = S_z;$$

$$I_{\pm 1} = \frac{\mp 1}{\sqrt{2}} (I_x \pm i I_y); \quad I_o = I_z$$

The spin operators have the property that

$$S^2 = \sum_{p=-1}^1 (-1)^p S_{-p} S_p = \sum_{p=-1}^1 S_p^\dagger S_p$$

Transformed into the rotating frame of the electron, the truncated Hamiltonian of eq 6 becomes

$$\tilde{H} = (\omega_o - \omega) S_o + \omega_n I_o + \bar{a} S_o I_o + \tilde{\epsilon}$$

$$\text{where } \tilde{\epsilon} = h \sum_{p=-1}^1 p S_p \left(\frac{(-1)^p}{\sqrt{2}} e^{ip\phi} \right) \quad (7)$$

In this rotating frame the Hamiltonian is independent of time. The equation of motion for the density matrix $\chi = \tilde{\rho} - \tilde{\rho}_o$ is

$$\dot{\chi} = -i[\tilde{H}, \chi] - R(\chi) - i[\tilde{\epsilon}, \tilde{\rho}_o] \quad (8)$$

$R(\chi)$ is the phenomenological Redfield relaxation operator whose form is given in the Appendix. The equilibrium density matrix, given by the Boltzmann equilibrium, is $\tilde{\rho}_o = e^{-H_o/kT}$. For any operator, O , there corresponds an observable, $\langle O \rangle = \text{tr}\{O\chi\}$, but whether it can be observed by the experiment at hand is another matter. The equations of motion from eq 8 can be rewritten as equations for observables:

$$\langle \dot{O} \rangle = -i\langle [O, \tilde{H}] \rangle - \langle R(O) \rangle - i\langle [O, \tilde{\epsilon}] \rangle_o \quad (9)$$

Equations 8 and 9 both contain the same information, and both are descriptions of the evolution of the system. However, there are important distinctions between them. Equation 8 is a modified form of a wave equation in which the elements of χ are basis set dependent. In contrast eq 9 is a description of the evolution of observable quantities. Observables are independent of the choice of basis vectors used to define the quantum mechanical system and truly represent classical equations of motion for observable quantities. As a result of this independence, for eq 9 any basis set is quite satisfactory. $\langle R(O) \rangle$

represents the effect of the relaxation on the operator O and is defined explicitly in eqs A-2A and A-2B in the Appendix. Evaluation of $\langle R(O) \rangle$ in terms of the CSA and the END mechanisms are shown in eq A-7 in the Appendix. Here, we need only consider them as phenomenological operators representing relaxation at some relaxation rate.

The evaluation of the commutators used in eq 9 can be accomplished by using the commutation rules for the spherical tensor operators:

$$[S_p, S_q] = s(q-p) S_{p+q} \quad (10)$$

where $s(n)$ is the signum of n . Using eq 10 for S (and the associated definitions for the I spin) along with the Hamiltonian of eq 7 in eq 8 or 9 results in the observables $\langle S_p \rangle$ only coupling among themselves and to one other set of observables, $\langle 2S_p I_o \rangle$, which represent other components of the magnetization.

It is possible to use a tensor basis set to make the definitions of the relaxation operations much easier to follow. The fundamental requirement of this set of basis matrices is that

$$\text{tr}\{T_q^k (T_{q'}^{k'})^\dagger\} = \delta_{k,k'} \delta_{q,q'}$$

For a spin $1/2$ particle, only rank $k = 0$ and $k = 1$ operators are needed. The $k = 0$ case (T_o^0) is just the identity operator. The $k = 1$ case gives a set of T_q^1 that are proportional to the S_q operators. For the case of two coupled, spin $1/2$ particles there are 16 elements in the density matrix, and this implies there exist 16 operators to span the space of those 16 elements. The set of 16 operators is generated from the direct product of the four operators for each spin, either

$$\{1, S_x, S_z, S_y\} \otimes \{1, I_x, I_z, I_y\} \quad \text{or} \\ \{1, S_{-1}, S_o, S_1\} \otimes \{1, I_{-1}, I_o, I_1\}$$

or

$$\{T(1)_o^0, T(1)_q^1\} * \{T(2)_o^0, T(2)_q^1\} \quad \text{or} \\ \{T(1,2)_o^0, T(1,2)_q^1, T(1,2)_q^2, T(1,2)_q^3\}$$

In terms of matrix representations, each of the single particle operators is 2×2 , and the 2 particle operators are 4 by 4. We use the independent particle set of operators to generate all 16 coupled observables. All frequency dependent terms in eq 8 can be evaluated using the fundamental relation that is given for tensor operators:¹⁵

$$[S_p, T(1)_q^k] = T(1)_q^k (-1)^{k-q'} \sqrt{k(k+1)(2k+1)} \begin{pmatrix} k & 1 & k \\ -q' & p & q \end{pmatrix} \quad (11)$$

where $q' = p + q$. There is a similar expression for $[I_p, T(2)_q^k]$.

Because of the similarity of the tensor and spin operators, we can consider the 16 operators to include one zero-spin operator (which does not couple to the observable), six single-spin operators $S_p 1, 1 I_q$, and nine two-spin operators of the form $2S_p I_q$.

The commutation terms from eq 9, using the stationary Hamiltonian in eq 7 are

$$\langle [\tilde{H}, S_q] \rangle = q \left(\Delta \langle S_q \rangle + \frac{\bar{a}}{2} \langle 2S_q I_o \rangle \right) + h \sum_{r=-1}^1 \langle S_{r+q} \rangle rs(r-q) \frac{1}{\sqrt{2}} e^{ir\phi} \quad (12A)$$

$$\langle [\tilde{H}, I_q] \rangle = q \left(\omega_n \langle I_q \rangle + \frac{\bar{a}}{2} \langle 2S_o I_q \rangle \right) \quad (12B)$$

$$\begin{aligned} \langle [\tilde{H}, 2S_q I_p] \rangle &= q \left(\Delta \langle 2S_q I_p \rangle + \delta_{p,o} \frac{\bar{a}}{2} \langle S_q \rangle \right) + \\ & p \left(\omega_n \langle 2S_q I_p \rangle + \delta_{q,o} \frac{\bar{a}}{2} \langle I_p \rangle \right) + h \sum_{r=-1}^1 \langle 2S_{r+q} I_p \rangle rs(r-q) \frac{1}{\sqrt{2}} e^{ir\phi} \end{aligned} \quad (12C)$$

where $\Delta = \omega_o - \omega$ is the resonance term. The important observables are contained in eqs 12A and 12C. The S_p operators ($p = +1, 0$, and -1) are coupled to each other and to operators of form $2S_p I_p$. The six most important observables are

$$\langle \vec{O} \rangle = \begin{pmatrix} \langle O_4 \rangle \\ \langle O_{12} \rangle \\ \langle O_2 \rangle \\ \langle O_{10} \rangle \\ \langle O_3 \rangle \\ \langle O_{11} \rangle \end{pmatrix} \equiv \begin{pmatrix} \langle S_{+1} \rangle \\ \langle 2S_{+1} I_o \rangle \\ \langle S_{-1} \rangle \\ \langle 2S_{-1} I_o \rangle \\ \langle S_o \rangle \\ \langle 2S_o I_o \rangle \end{pmatrix} \quad (12D)$$

[For a complete list of the operators O_j and definitions of the index j on O_j , see the Appendix.] The effect of the commutators with the Hamiltonian using the rules of eq 12 causes these observables to be coupled to one another by the 6×6 frequency matrix, Ω :

$$\begin{pmatrix} \langle [\tilde{H}, S_{+1}] \rangle \\ \langle [\tilde{H}, 2S_{+1} I_o] \rangle \\ \langle [\tilde{H}, S_{-1}] \rangle \\ \langle [\tilde{H}, 2S_{-1} I_o] \rangle \\ \langle [\tilde{H}, S_o] \rangle \\ \langle [\tilde{H}, 2S_o I_o] \rangle \end{pmatrix} = \Omega \begin{pmatrix} \langle S_{+1} \rangle \\ \langle 2S_{+1} I_o \rangle \\ \langle S_{-1} \rangle \\ \langle 2S_{-1} I_o \rangle \\ \langle S_o \rangle \\ \langle 2S_o I_o \rangle \end{pmatrix} \equiv \begin{pmatrix} \Delta & \frac{1}{2}\bar{a} & 0 & 0 & \frac{1}{\sqrt{2}}h & 0 \\ \frac{1}{2}\bar{a} & \Delta & 0 & 0 & 0 & \frac{1}{\sqrt{2}}h \\ 0 & 0 & -\Delta & -\frac{1}{2}\bar{a} & \frac{1}{\sqrt{2}}h & 0 \\ 0 & 0 & -\frac{1}{2}\bar{a} & -\Delta & 0 & \frac{1}{\sqrt{2}}h \\ \frac{1}{\sqrt{2}}h & 0 & \frac{1}{\sqrt{2}}h & 0 & 0 & 0 \\ 0 & \frac{1}{\sqrt{2}}h & 0 & \frac{1}{\sqrt{2}}h & 0 & 0 \end{pmatrix} \begin{pmatrix} \langle S_{+1} \rangle \\ \langle 2S_{+1} I_o \rangle \\ \langle S_{-1} \rangle \\ \langle 2S_{-1} I_o \rangle \\ \langle S_o \rangle \\ \langle 2S_o I_o \rangle \end{pmatrix} \quad (13)$$

The equilibrium magnetization terms in eq 9 that survive are

$$\langle [\tilde{\epsilon}, S_q] \rangle_o = \frac{\omega_o q^2 e^{iq\phi}}{\sqrt{2}kT} \quad \text{and} \quad \langle [\tilde{\epsilon}, 2S_q I_p] \rangle_o = \frac{\bar{a}}{4\omega_o} \delta_{p,o} \langle [\tilde{\epsilon}, S_q] \rangle_o \quad (14)$$

and produce the equilibrium magnetization column vector, \vec{Q} :

$$\vec{Q} = -\frac{\omega_o h}{kT} \begin{pmatrix} 1 \\ 0 \\ 1 \\ 0 \\ 0 \\ 0 \end{pmatrix}$$

Addition of relaxation operators, in a relaxation matrix \mathbf{R} , will further couple individual matrix elements (observables) to others. [The indices on the \mathbf{R} matrix elements are explained in the Appendix.] \mathbf{R} also shows how the six important elements, which are 4, 12, 2, 10, 3, and 11, relate to the relaxation:

$$\mathbf{R} = \begin{pmatrix} R^{4,4} & R^{4,12} & 0 & 0 & 0 & 0 \\ R^{12,4} & R^{12,12} & 0 & 0 & 0 & 0 \\ 0 & 0 & R^{2,2} & R^{2,10} & 0 & 0 \\ 0 & 0 & R^{10,2} & R^{10,10} & 0 & 0 \\ 0 & 0 & 0 & 0 & R^{3,3} & R^{3,11} \\ 0 & 0 & 0 & 0 & R^{11,3} & R^{11,11} \end{pmatrix} \equiv \begin{pmatrix} R_{2e} & R_{2x} & 0 & 0 & 0 & 0 \\ R_{2x} & R'_{2e} & 0 & 0 & 0 & 0 \\ 0 & 0 & R_{2e} & R_{2x} & 0 & 0 \\ 0 & 0 & R_{2x} & R'_{2e} & 0 & 0 \\ 0 & 0 & 0 & 0 & R_{1e} & R_{1x} \\ 0 & 0 & 0 & 0 & R_{1x} & R'_{1e} \end{pmatrix}$$

The fundamental rate of relaxation of a particular observable such as $\langle S_z \rangle \equiv \langle S_o \rangle$ is contained in the appropriate matrix element. For example, the spin-lattice relaxation rate, R_{1e} , is a relaxation matrix element that couples $\langle S_z \rangle$ to itself. $\langle S_z \rangle \equiv \langle S_o \rangle$ is the third element in the vector defining the set of observables and hence $R^{3,3} = R_{1e}$; similarly, the 11th element, the self-relaxation of $\langle 2S_o I_o \rangle$, is $R^{11,11} = R'_{1e}$. The calculation of the relaxation matrix requires us to consider the relaxation of the observables $\langle S_{+1} \rangle$ and $\langle 2S_{+1} I_o \rangle$ (elements 4 and 12 in the full matrix), which relax with rates R_{2e} and R'_{2e} , respectively. Matrix element 9, the nuclear magnetization observable $\langle I_o \rangle \equiv \langle I_z \rangle$, relaxes with rate R_{1n} . The details of the relaxation operators in \mathbf{R} , explicitly including the END and CSA Hamiltonians, are in the Appendix. Equation 5 in matrix form becomes

$$\dot{\langle \vec{O} \rangle} = -\{i\Omega + \mathbf{R}\} \langle \vec{O} \rangle + i\vec{Q} \quad (15)$$

where all terms have been defined. The formal general solution to this differential equation contains both the time domain, transient relaxing, signal $\langle \vec{O} \rangle(t)$ and the infinite time, steady state, CW signal $\langle \vec{O} \rangle(\infty)$:

$$\langle \vec{O} \rangle(t) - \langle \vec{O} \rangle(\infty) = e^{-\{i\Omega + \mathbf{R}\}t} (\langle \vec{O} \rangle(0) - \langle \vec{O} \rangle(\infty)) \quad (16)$$

where $\langle \vec{O} \rangle(\infty) = \{i\Omega + \mathbf{R}\}^{-1} i\vec{Q}$.

Examples

Recall that we wish to explain the discrepancy between the m dependent behavior of R_{2e} (the line widths in CW-EPR spectra) and the m independent spin–lattice relaxation R_{1e} . We present below two examples to illustrate how theory presented above addresses this apparent discrepancy. The first example—the linear CW-EPR experiment, which gives a line shape as a function of field—shows how the m dependent line widths arise in our form of the theory, which at present appears to contain no m dependence. The second example shows how the spin–lattice relaxation rates obtained in pulsed-SR and pulsed-ELDOR experiments are line independent, yet they arise from equations analogous to those for the m dependent line widths.

Linear Response CW-EPR Line Shape. The CW-EPR experimental observable is $\langle S_{+1} \rangle$. If we ignore the h terms in Ω (equivalent to carrying out the CW-EPR experiment well below saturation), then the only observable coupled to $\langle S_{+1} \rangle$ is $\langle 2S_{+1}I_o \rangle$ —and eq 13 is now in block diagonal form and the relevant part of the 6×6 matrix is only a 2×2 matrix. The steady state equation for $\langle S_{+1} \rangle$ becomes

$$\begin{pmatrix} i\Delta + R_{2e} & i\frac{\bar{a}}{2} + R_{2x} \\ i\frac{\bar{a}}{2} + R_{2x} & i\Delta + R'_{2e} \end{pmatrix} \begin{pmatrix} \langle S_{+1} \rangle \\ \langle 2S_{+1}I_o \rangle \end{pmatrix} = -\frac{i\omega_o h}{kT} \begin{pmatrix} 1 \\ 0 \end{pmatrix} \quad (17A)$$

The observable of interest $\langle S_{+1} \rangle$ contains, as a complex number, both the x and y components of the magnetization of the electron in the rotating frame, which is the CW-EPR signal. The solution of this equation gives the values of the two transverse components of the magnetization at infinite time; and by sweeping Δ a CW spectrum is produced.

How is it possible to have two Lorentzian lines with different widths from a set of equations that have no apparent dependence on m ? There is *no* manifold dependence in the definition of any of the elements of eq 17A. However, if we form the solution for $\langle S_{+1} \rangle$ by factoring out the diagonal term $i\Delta$ on left hand side of eq 17A and make use of the fact that, for this mechanism, the 2×2 rate matrix is independent of the sweep variable Δ , we get

$$\begin{bmatrix} i\Delta & 0 \\ 0 & i\Delta \end{bmatrix} + \begin{pmatrix} R_{2e} & i\frac{\bar{a}}{2} + R_{2x} \\ i\frac{\bar{a}}{2} + R_{2x} & R'_{2e} \end{pmatrix} \begin{pmatrix} \langle S_{+1} \rangle \\ \langle 2S_{+1}I_o \rangle \end{pmatrix} = -\frac{i\omega_o h}{kT} \begin{pmatrix} 1 \\ 0 \end{pmatrix} \quad (17B)$$

and diagonalizing this matrix problem gives the eigenvalues, λ_{\pm} :

$$\lambda_{\pm} = \frac{1}{2}(R_{2e} + R'_{2e}) \pm \sqrt{\left(\frac{1}{2}(R_{2e} - R'_{2e})\right)^2 + \left(i\frac{\bar{a}}{2} + R_{2x}\right)^2} \quad (18)$$

The observable is now the sum of two complex Lorentzian lines:

$$\langle S_{+1} \rangle = -i\frac{h\omega_o}{kT} \left\{ \frac{A_+}{i\Delta + \lambda_+} + \frac{A_-}{i\Delta + \lambda_-} \right\} \quad (19)$$

and the amplitudes, A_{\pm} , of the lines are

$$A_{\pm} = \frac{1}{2} \pm \frac{\frac{1}{2}(R_{2e} - R'_{2e})}{\sqrt{\left(\frac{1}{2}(R_{2e} - R'_{2e})\right)^2 + \left(i\frac{\bar{a}}{2} + R_{2x}\right)^2}} \quad (20)$$

(The equivalent for ^{14}N would result in three distinct eigenvalues and the diagonalization of a 3×3 matrix.) The interpretation of eqs 18–20 is remarkably simple if we neglect the $\frac{1}{2}(R_{2e} - R'_{2e})$ terms in the square roots of eqs 18 and 20 so that $\lambda_{\pm} \approx R_{2e} \pm (i\frac{\bar{a}}{2} + R_{2x})$ and $A_{\pm} = \frac{1}{2}$. We obtain two lines, the resonance positions of which occur at $\Delta \pm \bar{a}/2$, with equal amplitudes but different line widths, $R_{2e} \pm R_{2x}$, respectively. In *principle* both rates are simultaneously observed at all spectral positions. However, the presence of the resonance condition in the denominator of eq 19 ensures that only one of the two lines dominates the spectrum at any one position (as long as the splitting is larger than the relaxation rates, which is usually the case). The line splitting parameter, \bar{a} , is of crucial importance in spectrally resolving the two relaxation rates. The relaxation term, R_{2x} , is the rate responsible for the differences in line widths and comes from the cross correlation of the END and the CSA (see Appendix). Equation 18 can be rewritten in an m dependent form, $R_{2e}(m)$, using the real part of the eigenvalues, λ_{\pm} , viz.

$$R_{2e}(m) = \text{Real} \left\{ \frac{1}{2}(R_{2e} + R'_{2e}) + m\sqrt{(R_{2e} - R'_{2e})^2 + (i\bar{a} + 2R_{2x})^2} \right\} \quad \text{for } m = \pm 1/2 \quad (21)$$

Comparison with the $R_{2e}(m) \equiv T_{2e}^{-1}(m) = A + Bm + Cm^2$ formula of eq 1³ shows that the rates R_{2e} and R_{2x} as defined here, neglecting the $R_{2e} - R'_{2e}$ term, can be related to the A , B , and C parameters of eq 1 by $R_{2e} = A + \frac{1}{4}C$ and $R_{2x} = \frac{1}{2}B$. This shows how one can obtain two distinct resonance lines, with different line widths, from equations that apparently contain no manifold dependence. We should add that the form of the CW-EPR line shape given in eqs 18–20 encompasses a variety of well established physical phenomena including the following:

(i) emissive lines—When cross relaxation becomes large enough ($R_{2x} \gg R_{2e}$) the rate of relaxation of one of the lines will be negative; i.e., one of the lines will become emissive.

(ii) lines collapsing—When $|(R_{2e} - R'_{2e})| > \bar{a}$, then the two lines will begin to collapse to a single line in the center, regardless of the cross relaxation rate. Additional frequency shifts are contained in the imaginary parts of the eigenvalues of eq 18.

(iii) dynamic site hopping—Two-site dynamic hopping models, characterized by forward and backward hopping rates k_f and k_b are described by eqs 18–20 if $R_{2e} \equiv k_f + k_b$ and $R_{2x} \equiv k_f - k_b$.¹⁶

Pulsed Saturation Recovery and ELDOR. In time domain ELDOR experiments a strong microwave pulse is applied that induces a disturbance in the spin equilibrium. The system then relaxes back toward equilibrium in the presence of a very weak observing field, h . In the fast motion limit, eq 13 shows that the experimental observable $\langle S_{+1} \rangle$ is coupled only to 5 of the 16 observables: three transverse ones ($\langle S_{-1} \rangle$ and $\langle 2S_{\pm 1}I_o \rangle$) and two longitudinal ones ($\langle S_o \rangle$ and $\langle 2S_oI_o \rangle$). The pulse experiment is such that all transverse processes relaxing at R_{2e} (such as FIDs), are removed⁹ from the signal. Only terms proportional to the observer amplitude h are retained in the signal. In this section we compute expressions for the relaxation rates and then show that the longitudinal relaxation rates are carried over unchanged into the transverse magnetization detected experimentally.

Equation 16 shows that the system will relax back to its equilibrium position given an initial displacement, $\langle \Delta \vec{O} \rangle_o = \langle \vec{O} \rangle(0) - \langle \vec{O} \rangle(\infty)$, as

$$\langle \Delta \vec{O} \rangle(t) = \langle \vec{O} \rangle(t) - \langle \vec{O} \rangle(0) = e^{-\{i\Omega + R\}t} \langle \Delta \vec{O} \rangle_o \quad (22)$$

In this example $\langle\Delta\vec{O}\rangle(t)$ is the same 6×1 column vector on the right-hand side of eq 13 but with equilibrium (CW) components subtracted:

$$\langle\Delta\vec{O}\rangle(t) = \begin{pmatrix} \langle S_{+1} \rangle \\ \langle 2S_{+1}I_o \rangle \\ \langle S_{-1} \rangle \\ \langle 2S_{-1}I_o \rangle \\ \langle S_o \rangle - \langle S_o \rangle_\infty \\ \langle 2S_oI_o \rangle - \langle 2S_oI_o \rangle_\infty \end{pmatrix}$$

The frequency matrix, Ω , and the appropriate rate matrix, R , have been defined above. This assumes that there is no cross relaxation between the transverse and longitudinal components other than from the observer amplitude h , which is the case for the END and CSA mechanisms, as shown in the Appendix. When the observer amplitude is sufficiently small, then the Ω matrix of eq 13 becomes

$$\Omega = \begin{pmatrix} \Delta & \frac{1}{2}\vec{a} & 0 & 0 & 0 & 0 \\ \frac{1}{2}\vec{a} & \Delta & 0 & 0 & 0 & 0 \\ 0 & 0 & -\Delta & -\frac{1}{2}\vec{a} & 0 & 0 \\ 0 & 0 & -\frac{1}{2}\vec{a} & -\Delta & 0 & 0 \\ 0 & 0 & 0 & 0 & 0 & 0 \\ 0 & 0 & 0 & 0 & 0 & 0 \end{pmatrix}$$

and eq 16 then partitions into a 4×4 matrix and a 2×2 matrix:

$$\langle\Delta\vec{O}_2\rangle(t) = \begin{pmatrix} \langle S_{+1} \rangle \\ \langle 2S_{+1}I_o \rangle \\ \langle S_{-1} \rangle \\ \langle 2S_{-1}I_o \rangle \end{pmatrix} \quad \text{and} \quad \langle\Delta\vec{O}_1\rangle(t) = \begin{pmatrix} \langle S_o \rangle - \langle S_o \rangle_\infty \\ 2(\langle S_oI_o \rangle - \langle S_oI_o \rangle_\infty) \end{pmatrix}$$

The two longitudinal components of the magnetization $\langle\Delta\vec{O}_1\rangle(t)$ therefore relax to equilibrium on their own with the form:

$$\langle S_z \rangle(t) - \langle S_z \rangle_o = B_+ e^{-R_+^1 t} + B_- e^{-R_-^1 t} \quad (23)$$

The effective relaxation rates are

$$R_\pm^1 = \frac{1}{2}(R_{1e} + R'_{1e}) \pm \sqrt{\left(\frac{1}{2}(R_{1e} - R'_{1e})\right)^2 + (R_{1x})^2} \quad (24)$$

These two equations for R_\pm^1 differ from their $R_{2e}(m)$ counterparts in having no term in \vec{a} so that *both rates are independent of line position and the amplitudes are always large*. The amplitudes, B_\pm , are determined by the initial pulse conditions and are approximately equal.

This point can be made more clearly if we Fourier transform (FT) the CW-EPR signal (eq 19) into the time domain and compare this with eq 23. The FT of eq 19 is

$$\langle S_{+1} \rangle = i \frac{h\omega_o}{kT} \{A_+ e^{-i\lambda_+} + A_- e^{-i\lambda_-}\} \quad (25)$$

The amplitudes A_\pm approximately equal the B_\pm . What makes eqs 23 and 25 different is that the spin-lattice rates of eq 23,

R_\pm^1 , are real, but the spin-spin rates, λ_\pm , are complex, because the λ_\pm have frequency terms that oscillate at frequencies $\pm\vec{a}/2$. These oscillations of the λ_\pm signals at two *different* frequencies in the time domain means that in the frequency/field domain (i.e., the CW EPR experiment) these two components are separated and appear in the spectrum in different positions. In contrast, the spin-lattice relaxation rates are real at all frequencies, and hence both contribute to each line. A statement that says “ R_{2e} is strongly dependent on the line observed but R_{1e} is not” is therefore somewhat misleading. In CW measurements there are *two* spin-spin relaxation rates and in time domain EPR there are *two* spin-lattice relaxation rates. The distinction is that both spin-lattice rates are simultaneously observed in pulsed-SR and pulsed-ELDOR experiments, while in CW-EPR only one of the two spin-spin rates dominates at any particular spectral position due to the large \vec{a} in the expressions for R_{2e} .

Longitudinal Relaxation and the Pulsed ELDOR Signal

In this section we clarify how the longitudinal components discussed in eqs 23–24 enter into the transverse magnetization signal. $\langle S_{+1} \rangle$ is the observed signal and is generally recorded under conditions of low observer amplitude. As noted, this low observer amplitude allows a partitioning of the matrices of eqs 15 and 16 into transverse and longitudinal components. The frequency and relaxation matrix can be similarly partitioned:

$$i\Omega + R = \begin{pmatrix} \mathbf{A}_2 & h\mathbf{B} \\ h\mathbf{B}^t & \mathbf{A}_1 \end{pmatrix}$$

where \mathbf{A}_2 is a 4 by 4 matrix:

$$\mathbf{A}_2 = i \begin{pmatrix} \Delta & \frac{1}{2}\vec{a} & 0 & 0 \\ \frac{1}{2}\vec{a} & \Delta & 0 & 0 \\ 0 & 0 & -\Delta & -\frac{1}{2}\vec{a} \\ 0 & 0 & -\frac{1}{2}\vec{a} & -\Delta \end{pmatrix} + \begin{pmatrix} R_{2e} & R_{2x} & 0 & 0 \\ R_{2x} & R_{2e} & 0 & 0 \\ 0 & 0 & R_{2e} & R_{2x} \\ 0 & 0 & R_{2x} & R_{2e} \end{pmatrix}$$

\mathbf{A}_1 is a 2 by 2 matrix:

$$\mathbf{A}_1 = \begin{pmatrix} R_{1e} & R_{1x} \\ R_{1x} & R_{1e} \end{pmatrix}$$

and \mathbf{B} is the 2×4 matrix which when $h \neq 0$ allows coupling between longitudinal and transverse components:

$$\mathbf{B} = \frac{i}{\sqrt{2}} \begin{pmatrix} 1 & 0 \\ 0 & 1 \\ 1 & 0 \\ 0 & 1 \end{pmatrix}$$

Equation 16, which describes the evolution of the spin system, can be written as

$$\begin{pmatrix} \langle\Delta\vec{O}_2\rangle \\ \langle\Delta\vec{O}_1\rangle \end{pmatrix}(t) = \exp \left[- \begin{pmatrix} \mathbf{A}_2 & h\mathbf{B} \\ h\mathbf{B}^t & \mathbf{A}_1 \end{pmatrix} t \right] \begin{pmatrix} \langle\Delta\vec{O}_2\rangle_o \\ \langle\Delta\vec{O}_1\rangle_o \end{pmatrix} \quad (26)$$

With no loss of generality, the matrix in the exponential can be

diagonalized by a unitary transformation using the **T** and **U** transformation matrices:

$$\begin{pmatrix} \mathbf{T}_2^{-1} & \mathbf{U}_{12} \\ \mathbf{U}_{21} & \mathbf{T}_1^{-1} \end{pmatrix} \begin{pmatrix} \mathbf{A}_2 & h\mathbf{B} \\ h\mathbf{B}^\dagger & \mathbf{A}_1 \end{pmatrix} \begin{pmatrix} \mathbf{T}_2 & \mathbf{T}_{12} \\ \mathbf{T}_{21} & \mathbf{T}_1 \end{pmatrix} = \begin{pmatrix} \mathbf{A}_2 & 0 \\ 0 & \mathbf{A}_1 \end{pmatrix}$$

so that

$$\begin{pmatrix} \langle \Delta \tilde{O}_2 \rangle \\ \langle \Delta \tilde{O}_1 \rangle \end{pmatrix}(t) = \begin{pmatrix} \mathbf{T}_2 & \mathbf{T}_{12} \\ \mathbf{T}_{21} & \mathbf{T}_1 \end{pmatrix} \times \exp \left[- \begin{bmatrix} \Lambda_2 & 0 \\ 0 & \Lambda_1 \end{bmatrix} t \right] \begin{pmatrix} \mathbf{T}_2^{-1} & \mathbf{U}_{12} \\ \mathbf{U}_{21} & \mathbf{T}_1^{-1} \end{pmatrix} \cdot \begin{pmatrix} \langle \Delta \tilde{O}_2 \rangle_o \\ \langle \Delta \tilde{O}_1 \rangle_o \end{pmatrix} \quad (27)$$

Furthermore, we can diagonalize the two submatrices, **A**₁ and **A**₂ independently when the field amplitude, *h*, is small:

$$\mathbf{T}_2^{-1} \mathbf{A}_2 \mathbf{T}_2 = \Lambda_2 \quad \text{and} \quad \mathbf{T}_1^\dagger \mathbf{A}_1 \mathbf{T}_1 = \Lambda_1$$

The requirement that the diagonalized matrix have zero off-diagonal elements in eq 27 leads to conditions that connect the elements of the **T** and **U** transformation matrices: e.g., to first order in *h*, element **U**₁₂ must obey the condition that

$$\mathbf{U}_{12} = -\mathbf{T}_2^{-1} \mathbf{T}_{12} \mathbf{T}_1^{-1}$$

because the product of the **T** matrix and its inverse must be unity:

$$\begin{pmatrix} \mathbf{T}_2^{-1} & \mathbf{U}_{12} \\ \mathbf{U}_{21} & \mathbf{T}_1^{-1} \end{pmatrix} \begin{pmatrix} \mathbf{T}_2 & \mathbf{T}_{12} \\ \mathbf{T}_{21} & \mathbf{T}_1 \end{pmatrix} = \begin{pmatrix} 1 & 0 \\ 0 & 1 \end{pmatrix}$$

Similarly, to first order in *h* a requirement on **T**₁₂ is that: **T**₁₂**A**₁ − **A**₂**T**₁₂ = *h***B****T**₁ so that **T**₁₂ is proportional to the field amplitude, *h*. These results mean that the off diagonal elements, **U**₁₂ and **U**₂₁ are proportional to the off diagonal elements **T**₁₂ and **T**₂₁, so that all four elements are proportional to *h*. Evaluating eq 27 results in $\langle \Delta O_2 \rangle(t)$ being composed of four terms:

$$\langle \Delta O_2 \rangle(t) = e^{-i\Lambda_2 t} \langle \Delta O_2 \rangle_o - e^{-i\Lambda_2 t} \mathbf{T}_{12} \mathbf{T}_1^{-1} \langle \Delta O_1 \rangle_o + \mathbf{T}_{12} e^{-i\Lambda_1 t} \mathbf{T}_1^{-1} \langle \Delta O_1 \rangle_o - \mathbf{T}_{12} e^{-i\Lambda_1 t} \mathbf{U}_{12} \langle \Delta O_2 \rangle_o \quad (28)$$

The first term in eq 28 is the FID of the transverse components; the second term is generated by a population difference of the longitudinal components and decays at the same rate as the transverse components. This signal produces FID-like oscillations whose amplitudes are proportional to *h*, but they are not Torrey oscillations because the oscillation frequency does not depend on *h*.¹⁷ The final term is second order in *h* (because **T**₁₂ and **U**₁₂ are each proportional to *h*) and therefore contributes very little to the signal. The third term in eq 28 (1) is proportional to the population deviation induced by the pulse, (2) relaxes at the rates of the longitudinal components, and (3) is linear in *h*. This fits all the requirements to be either a pulsed-SR or a pulsed-ELDOR signal. The rates in **A**₁ are the R_\pm^1 as defined in eq 24 and do not depend on spectral position. The matrix **T**₁₂ multiplying the **A**₁ matrix is a function of field position via the dependence of **T**₁₂ on **A**₂, so that the amplitudes of the two exponential decays may depend on field position but the decay rates themselves do not. We have assumed throughout that the relaxation matrix couples $\langle S_o \rangle$ only to $\langle 2I_o S_o \rangle$; although, in general, the relaxation matrix may couple $\langle S_o \rangle$ with

other observables. For example, cross relaxation from $\langle S_o \rangle$ to $\langle I_o \rangle$, which is an important term in the dynamic Overhauser effect,¹¹ is neglected in this treatment.

Results

We use the theory explicitly developed in the Appendix to generate results in the form of plots of relaxation rates vs rotational correlation time using the END and CSA Hamiltonians as the only sources of relaxation. The dynamics process is isotropic, rotational Brownian motion. Equations 21 and 24 defining the relaxation rates can be written in terms of specific matrix elements of **R** for the two spin–spin relaxation rates as

$$R_\pm^{2e} = \frac{1}{2}(R^{4,4} + R^{12,12}) \pm \text{Re} \left\{ \sqrt{\left(\frac{1}{2}(R^{4,4} - R^{12,12}) \right)^2 + \left(\bar{a} - R^{4,12} \right)^2} \right\}$$

and for the two spin–lattice relaxation rates as

$$R_\pm^{1e} = \frac{1}{2}(R^{3,3} + R^{11,11}) \pm \sqrt{\left(\frac{1}{2}(R^{3,3} - R^{11,11}) \right)^2 + (R^{3,11})^2}$$

The individual elements are computed using eq A-7 in the Appendix:

$$R^{ij} = \sigma_{aa}^2 \sum_{m,n=-1}^1 C_{n,m}^{ij} J_{n,m} + \sigma_{gg}^2 \sum_{n=-1}^1 C_n^{ij} J_{n,o} + \sigma_{ag}^2 \sum_{m,n=-1}^1 C_{n,m}^{ij} J_{n,m}$$

where the $J_{n,m}$ are the spectral density functions and the $C_{n,m}^{ij}$ are dimensionless coefficients on the order of unity, defined in the Appendix. The variances, σ_{aa}^2 , are defined in the Appendix. We have neglected spin rotation, spin diffusion, and other bimolecular collision-induced relaxation mechanisms for the sake of simplicity. Inclusion of them is straightforward and simply additive. None of these mechanisms introduces new cross correlations and therefore their neglect does not qualitatively change the results presented here.

In Figure 2 we show the results for the spin–spin relaxation rates R_{2e} (relaxation matrix element $R^{4,4}$, lower dotted line), R'_{2e} ($R^{12,12}$, upper dotted line), and the cross term R_{2x} ($R^{4,12}$, dashed line) which couples R_{2e} to R'_{2e} , i.e., element 4,4 to 12,-12. The effect of the cross term R_{2x} is to make the smaller rate slightly smaller and the larger rate slightly larger, as predicted in eq 21. The $R_{2e}(m)$ for $m = +1/2$ defined in eq 21 are shown as the two solid lines; the circles and \times 's are the relaxation rates calculated from the equations of Hwang et al.³ and are identical with our rates. $A + 1/4C$ (as defined by Hwang³) is identical to $1/2(R_{2e} + R'_{2e})$ and $B \cong 2R_x$.

Figure 3 is a plot of the fundamental rates R_{1e} , $2W_e$, R_{1x} , R_{1n} , and R'_{1e} as functions of the rotational correlation time τ_c . R_{1e} , $2W_e$, and R_{1x} are dominated by a single spectral density function that peaks as a function of τ_c at $\tau_c \approx 2 \times 10^{-11}$ s, when $\omega_o \tau_c = 1$. R_{1n} and R'_{1e} are likewise dominated by a single spectral density function that peaks at $\tau_c \approx 10^{-8}$ s when $(\bar{a}/2)\tau_c = 1$. These results follow from the END mechanism and have been observed experimentally over a wide range of correlation times.⁹ These results also agree with the data of Hyde et al.¹⁸ for those data for which instrumental limitations did not cause artifacts.

Figure 4 shows the experimentally observable rates $R_1(\pm)$ from eq 24 (pair of solid lines) and R_{1e} (dashed line) and $(R_{1e}$

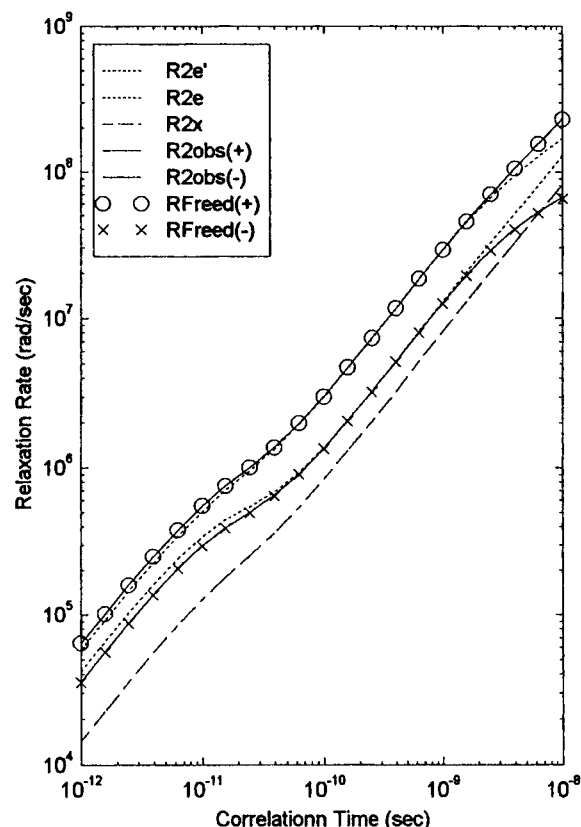


Figure 2. Spin-spin relaxation rates R_{2e} , R'_{2e} (dotted lines) with $R'_{2e} > R_{2e}$ and the cross term R_{2x} (dashed line) which couples them are shown as functions of rotational correlation time, τ_c , used in eq 18. The observable rates $R_{2e}(\pm)$ for $m = \pm 1/2$ are shown as solid lines; superimposed are the line widths (as rates) $R_{\text{Free}}(\pm)$ calculated from eq 13 shown as circles ($m = +1/2$) and x's ($m = -1/2$), respectively.

+ R_{1n}) (dotted line) versus rotational correlation time calculated using eq A-7 in the Appendix. The effect of the nonzero R_{1x} cross relaxation process is to add and subtract from the fundamental rates R_{1e} and R'_{1e} to produce the two observable rates $R_1(\pm)$. For correlation times where $\omega_0\tau_c > 5$ (on the long τ_c side of the R_{1e} spectral density function) eq 24 gives approximately that $R_1(+)$ $\approx R'_{1e} \approx R_{1e} + R_{1n}$ and $R_1(-)$ $\approx R_{1e}$. In prior publications⁹ $R_1(+)$ was identified with the sum of R_{1e} and R_{1n} . Figure 4 shows that this assumption is reasonable only for long correlation times. This is not the case in the fast motion limit ($\omega_0\tau_c < 1$): In this region $R'_{1e} < R_{1e} \approx R_{1n}$, and the slower observable rate $R_1(-)$ cannot be labeled as being the true "spin-lattice relaxation rate" and is about a factor of 2 smaller than R_{1e} . $R_1(+)$ is about a factor of 2 smaller than $(R_{1e} + R_{1n})$.

Figure 5 presents plots of $b = W_n/W_e$ and $b' = W_x/W_e$ as functions of τ_c in order to obtain results in a form compatible with the Solomon 4-level picture used in the Introduction. The values of b and b' were computed from eq 5. For $\omega_0\tau_c < 1$ b is of order unity but steadily increases to a maximum of about 10^5 when $(\bar{a}/2)\tau_c \approx 1$. Because W_x and W_e have a similar dependence upon the correlation time, b' is nearly constant and ~ 2 over the entire motional range. This is the logical consequence of using the END and CSA Hamiltonians. These results compare favorably with other systems in which both W_e and W_x have been measured.¹⁹ From eq 4 the electron spin-lattice relaxation rate is $R_{1e} = 2W_e(1 + b') \approx 6W_e$ taking into account all possible pathways.

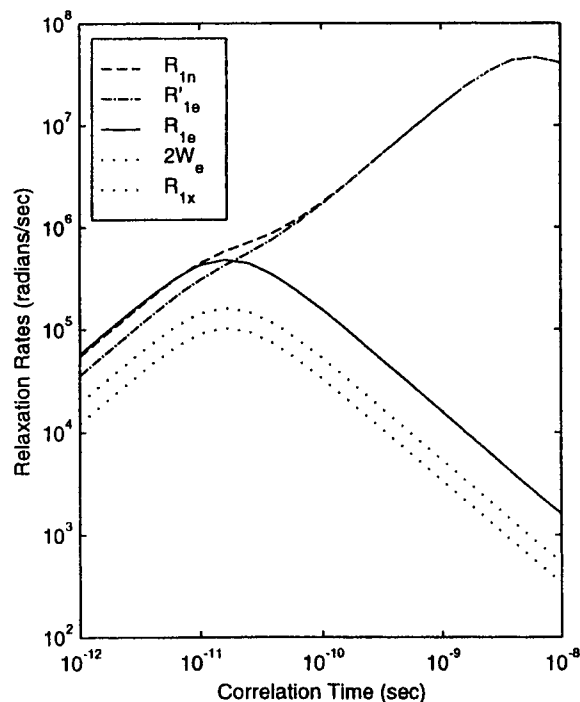


Figure 3. Plot of the fundamental rates R_{1n} , R'_{1e} , R_{1e} , $2W_e$, and R_{1x} as functions of the rotational correlation time. The three rates R_{1e} (solid line), $2W_e$ (top dotted line), and R_{1x} (lowest dotted line) are in descending order ($R_{1e} > 2W_e > R_{1x}$) and are dominated by a single spectral density function that peaks at $\tau_c \approx 2 \times 10^{-11}$ s when $\omega_0\tau_c = 1$ for the EPR spectrometer frequency of 9 GHz. R'_{1e} (dash-dot line) and R_{1n} (dashed line) are likewise dominated by a single spectral density function that peaks at $(\bar{a}/2)\tau_c = 1$ ($\tau_c \approx 2 \times 10^{-8}$ s). The rates R_{1e} and R'_{1e} are equal at $\omega_0\tau_c = 1$, and the curves cross at this point.

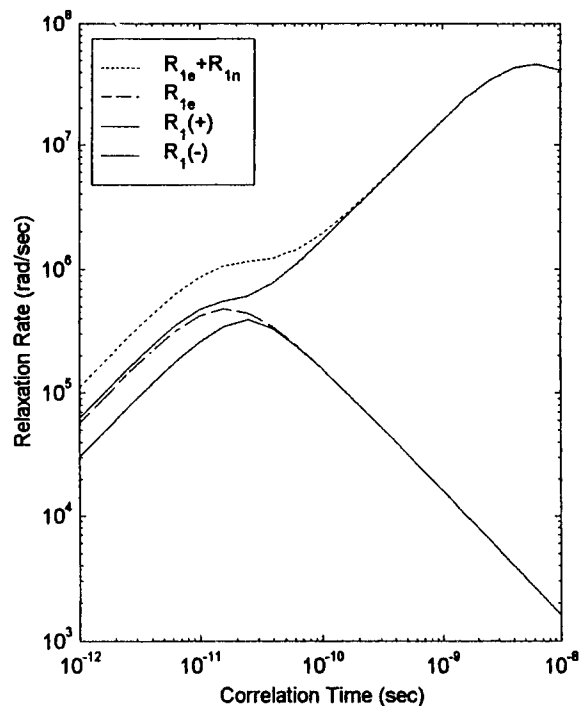


Figure 4. The two observable rates $R_1(\pm)$ (solid lines) are plotted as functions of the rotational correlation time. For comparison, R_{1e} (dashed line) and $R_{1e} + R_{1n}$ (dotted line) are also plotted.

Conclusions

The most important result of this paper is that a single theoretical approach provides clarification of the manifold dependencies of relaxation rates, viz., why the spin-spin

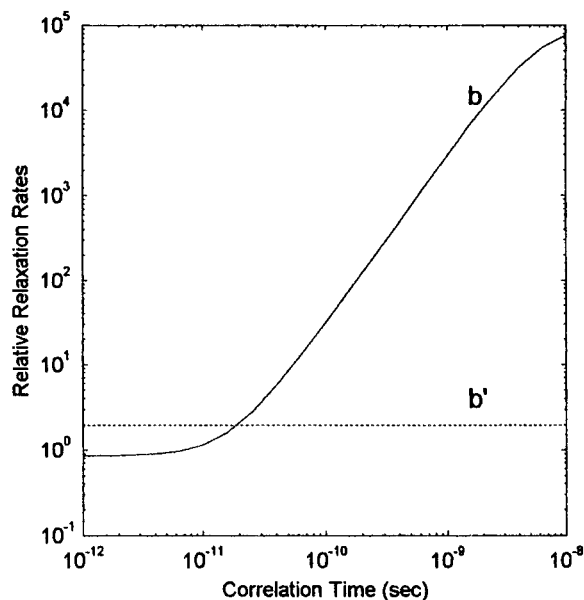


Figure 5. Plots of $b = W_n/W_e$ (solid line) and $b' = W_x/W_e$ (dotted line) as functions of rotational correlation time. The values of b and b' were computed from the rates in eq 24 with eq 5. Note that b' is ~ 2 over the entire motional range.

dephasing relaxation rates are nuclear manifold dependent but spin–lattice relaxation rates are independent of nuclear manifold. We have developed a formalism that depended on the observables as a function of the resonance field and the resonance condition. In our treatment, the set of magnetic resonance equations is cast in the form of coupled observables that have no particular association with any specific nuclear spin, m . The relaxation processes can be specified in terms of observables, allowing one to directly label relaxation rates in terms of observables that are relaxed.

The approach taken here leads to results virtually identical to those of Freed and Kivelson for R_{2e} processes and explains the experimentally observed m independence of the spin–lattice relaxation. There are two reasons for the different behaviors of R_{1e} and R_{2e} . The first is that the spin–spin relaxation rates are different because of the existence of cross relaxation rates generated by the END-CSA cross correlation. Secondly, the spin–lattice relaxation rates are not coupled by cross terms that depend upon the resonance conditions. Cross relaxation rates may be just as important in defining the relaxation of the longitudinal components as they are for the transverse components, but there is no possibility that the relaxation rates can be field position dependent because there is no term of the form $R_{1e} \pm i\bar{a}/2$. The *rates* do not depend on the resonance positions but the *amplitudes* of these components definitely can and do depend on the resonance positions (as well as the experimental initial pulse conditions).

Our choice of mechanisms does not limit the picture presented here. We considered the relaxation generated only by CSA and END and their cross correlation. Other mechanisms, such as spin rotation or spin diffusion (or any general spin angular momentum coupling) only contribute to relaxation of the diagonal elements of the relaxation matrix. Restricting the motional process to isotropic Brownian diffusion only puts a particular dependence on correlation time of the rates but otherwise is not an important factor. In systems of high viscosity, where the dynamics of relaxation no longer fully average the EPR spectrum, one can have a position dependent relaxation rate, but not a manifold dependent one.²⁰ Other, more compli-

cated mechanisms and Hamiltonians must be introduced to obtain true manifold dependent relaxation rates.

Acknowledgment. We wish to thank NIEHS for spectrometer support and NIH for support (GM32681) and for a training grant to A.W.R.

Appendix

The dominant Hamiltonians incorporated into relaxation mechanisms for spin labels are the END (electron–nuclear dipolar coupling) and the CSA (chemical shift anisotropy or g-tensor) Hamiltonians. The spin-rotation mechanism, and electron interaction with solvent spins and oxygen are also important, but they will not be dealt with explicitly here. In this Appendix we wish to give the relaxation terms primarily responsible for relaxation in liquids for spin labels. We have recast the theory as developed by Abragam to include END and CSA terms and the cross relaxation in terms of the observables.

General Equations for Relaxation. The density matrix equation in the laboratory frame may be written to include a relaxation process. This is done by defining a motion independent Hamiltonian as $H_o = \bar{H}$ where the bar represents averaging over the stochastic motional process. The rest of the Hamiltonian is rotating in the frame of the motion independent Hamiltonian: $H^x(t) = e^{-iH_o t} \{H - H_o\} e^{+iH_o t}$. $H^x(t)$ is in the interaction frame. The density matrix equation of motion for the system, to first order in the fluctuating terms, (the Redfield approximation¹⁰) is given as

$$\dot{\bar{\chi}} = -i[H_o + \epsilon, \bar{\chi}] - i[\epsilon, \bar{\rho}_o] - \int_{\tau=0}^{\infty} \{ [H^x(0)[H^x(\tau), \bar{\chi}(\tau)] \} d\tau \quad (\text{A-1})$$

All terms in eq A-1 can be transformed into a rotating frame in which the rotation rate is at the rf frequency. Such a transformation has the effect of making ϵ stationary. The rotation can be into a frame in which only the electron rotates, in that case, $U(t) = e^{-i\omega S_o t}$ serves as the rotation operation. Alternatively, the rotation can be into a frame in which both spins are rotating, in which case $U(t) = e^{-i\omega(S_o + I_o)t}$. The equations of motion must, of course, yield identical results, independent of frame. As the rest of the theory is in a rotating frame the tilde notation will not be explicitly shown hereafter.

Equation A-1 can be converted in an equation of motion for an observable $\langle O_j \rangle$. The observable associated with operator O_j is given by $\langle O_j \rangle(t) = \text{tr}\{O_j \bar{\chi}(t)\}$, where the density matrix may be in any frame. It is possible to construct a set of operators such that $\text{tr}\{O_k O_j^\dagger\} = \delta_{kj}$. Then the density matrix may be expanded such that: $\bar{\chi} = \sum_{j=1}^{n^2} O_j^\dagger \langle O_j \rangle$. For an n by n density matrix there are n^2 operators. The density matrix equation above, (A-1), then becomes a set of coupled equations for the operators:

$$\begin{aligned} \dot{\langle O_j \rangle} = & -i \sum_k \langle O_k \rangle \text{tr}\{O_j [H_o, O_k^\dagger]\} - i[\langle O_j, \epsilon \rangle]_o - \\ & \sum_k \langle O_k \rangle \int_{\tau=0}^{\infty} \text{tr}\{[O_j, H^x(0)][H^x(\tau), O_k^\dagger]\} d\tau \quad (\text{A-2A}) \end{aligned}$$

TABLE 1: Definition of Symbols α_{2p} and γ_{2p} Used in Eq A-3 of the Appendix

p	0	+1, -1	+2, -2
α_p	$(a_z - \bar{a})\sqrt{30/4}$	0	$(a_x - a_y)\sqrt{5/4}$
γ_p	$\omega_o((g_z - \bar{g})/\bar{g})\sqrt{30/4}$	0	$\omega_o((g_x - g_y)/\bar{g})\sqrt{5/4}$

The last expression in eq A-2 couples observable $\langle O_j \rangle$ to $\langle O_k \rangle$ and represents the relaxation rate constants R^{jk} between the two observables:

$$R^{jk} = \int_{\tau=0}^{\infty} \text{tr}\{[O_j, H^x(0)][H^x(\tau), O_k^\dagger]\} d\tau \quad (\text{A-2B})$$

We shall use the independent particle operators as a complete set of operators, as discussed in the text, normalized so that the matrix orthonormality condition, $\text{tr}\{O_k O_j^\dagger\} = \delta_{kj}$, holds. We now have a form that can be used to directly calculate all relaxation rates for any specific Hamiltonian. Specifically, the dipolar END and CSA Hamiltonians may be grouped together to give a single Hamiltonian in the interaction frame:

$$H^x(\tau) = \sum_{m,n=-1}^1 \{\tilde{A}_{n,m} \sum_{p=-1}^1 \alpha_{2p} \mathcal{D}_{2p,q}^2(\Omega) + \tilde{A}_n \delta_{m,0} \sum_{p=-1}^1 \gamma_{2p} \mathcal{D}_{p,-n}^2(\Omega)\} \quad (\text{A-3})$$

where $q = -(n + m)$ and the spin operators A are

$$\tilde{A}_n = \tilde{S}_n \begin{pmatrix} 1 & 1 & 2 \\ 0 & n & -n \end{pmatrix} \quad \text{and} \quad \tilde{A}_{n,m} = \tilde{S}_n \tilde{I}_m \begin{pmatrix} 1 & 1 & 2 \\ m & n & q \end{pmatrix} \quad (\text{A-4})$$

See also Table 1. The operators in the interaction frame of the zeroth-order Hamiltonian are approximately related to the stationary operators by

$$\begin{aligned} \tilde{A}_n &= A_n e^{-i\omega_o \tau} \cos(n\tau\bar{a}/2) = A_n f_{n,0}(\tau) \\ \tilde{A}_{n,m} &= A_{n,m} e^{-i\omega_o \tau} \cos(n\tau\bar{a}/2) e^{-i\omega_n \tau} \cos(m\tau\bar{a}/2) = \\ &A_{n,m} f_{n,m}(\tau) \quad (\text{A-5}) \end{aligned}$$

The elements of \mathbf{A} in the frame rotating with the zeroth-order Hamiltonian given as $H_o = \omega_o S_o + \omega_n I_o + \bar{a} S_o I_o$ are defined somewhat differently from Abragam.¹¹ Here, they are merely products of individual operators and not the sums of products given by Abragam,¹¹ (Chapter VIII, and elsewhere). The first index in the two-index terms for both \mathbf{A} and f refer to the electron operator, and the second index refers to the nuclear operator. The single indexed operators A_n refer to the electron only. Direct substitution of eq A-3 into eq A-2 gives a general expression for the relaxation process: For example the END term alone will give

$$R_{\text{end}}^{ij} = \sum_{m,n,m',n'=-1}^1 \text{tr}\{[O_i, A_{n,m}][A_{n',m'} O_j^\dagger]\} \times \sum_{p,p'=-1}^1 \alpha_{2p} \alpha_{2p'} \int_{\tau=0}^{\infty} f_{n',m'}(\tau) \overline{\mathcal{D}_{2p,q}^2(\Omega) \mathcal{D}_{2p',q'}^2(\Omega(\tau))} d\tau \quad (\text{A-6})$$

The averaging over any motional process which fully decorrelates the orientation variables (the case of freely rotating bodies

TABLE 2: 3-j Symbols Used $\begin{pmatrix} 1 & 1 & 2 \\ m & n & q \end{pmatrix}$ as a Function of m and n , Where $m + n + q = 0$

$n =$	+1	0	-1	m
$\begin{pmatrix} 1 & 1 & 2 \\ m & n & q \end{pmatrix} = \frac{1}{\sqrt{5}} \begin{bmatrix} 1/\sqrt{6} & -1/\sqrt{2} & 1 \\ -1/\sqrt{2} & \sqrt{2/3} & -1/\sqrt{2} \\ 1 & -1/\sqrt{2} & 1/\sqrt{6} \end{bmatrix}$	-1	0	+1	

in viscous media) satisfies the conditions that $q = -q'$, where $q = -(m + n)$, and $q' = -(m' + n')$ for the operator indices $\{m, n, m', n'\}$ that take on values of 0 or ± 1 . See Table 2.

The orientation dependent averaging is very simple for isotropic rotational Brownian dynamics, which is characterized by a single correlation time $\tau_c = 1/6D$, where D is the Stokes–Einstein–Debye rotational diffusion coefficient. In this circumstance:

$$\overline{\mathcal{D}_{2p,q}^2(\Omega) \mathcal{D}_{2p',q'}^2(\Omega(\tau))} = \frac{1}{5} (-1)^q \delta_{p,-p'} \delta_{q,-q'} e^{-\tau/\tau_c}$$

This vastly simplifies the sums so that

$$\begin{aligned} \sum_{p,p'=-1}^1 \alpha_{2p} \alpha_{2p'} \overline{\mathcal{D}_{2p,q}^2(\Omega) \mathcal{D}_{2p',q'}^2(\Omega(\tau))} = \\ \frac{1}{5} (-1)^q \delta_{q,-q'} e^{-\tau/\tau_c} \sum_{p=-1}^1 \alpha_{2p}^2 \end{aligned}$$

The sum can be reduced to a related sum in terms of the tensor elements:

$$\sigma_{\text{aa}}^2 = \frac{1}{5} \sum_{p=-1}^1 \alpha_{2p}^2 = \sum_{i=1}^3 (a_i - \bar{a})^2$$

One can define a variance for the \mathbf{g} tensor and a covariance between the \mathbf{A} and \mathbf{g} tensors as

$$\begin{aligned} \sigma_{\text{gg}}^2 &= \frac{1}{5} \sum_{p=-1}^1 \gamma_{2p}^2 = \left(\frac{\omega_o}{\bar{g}}\right)^2 \sum_{i=1}^3 (g_i - \bar{g})^2 \\ \sigma_{\text{ag}}^2 &= \frac{1}{5} \sum_{p=-1}^1 \alpha_{2p} \gamma_{2p} = \left(\frac{\omega_o}{\bar{g}}\right) \sum_{i=1}^3 (a_i - \bar{a})(g_i - \bar{g}) \end{aligned}$$

All three of these variances are rotationally invariant; i.e., these sums are independent of the coordinate system in which the tensors are defined. It has been assumed that the \mathbf{a} and \mathbf{g} tensors are collinear—an excellent approximation for spin labels.

The Fourier transform of the correlation function for the different relaxation frequencies is

$$J_{n,m} = \int_{\tau=0}^{\infty} f_{n,m}(\tau) e^{-\tau/\tau_c} d\tau = \tau_c \sum_{k=1}^4 \frac{1}{1 + i\{\omega_o + m\omega_n + \omega_k\}\tau_c}$$

where we define all four possible values of ω_k :

$$\begin{pmatrix} \omega_1 \\ \omega_2 \\ \omega_3 \\ \omega_4 \end{pmatrix} = \frac{\bar{a}}{2} \begin{pmatrix} n + m \\ m - n \\ n - m \\ -(n + m) \end{pmatrix}$$

In the fast motion limit the Fourier transforms all become the correlation time $J_{m,n} = \tau_c$. The general symmetry of this spectral density function is $J_{m,n} = J_{-m,-n}^*$. For purposes of defining relaxation processes, generally only the real part of J is retained (an approximation made in Chapter VIII of Abragam¹¹). $\text{Re}\{J_{m,n}\} = \text{Re}\{J_{-m,-n}\}$ is the only needed symmetry. With the help of these definitions the relaxation rates can be written as the sum of the END and the CSA terms plus END-CSA cross terms:

$$R^{ij} = \sigma_{\text{aa}}^2 \sum_{m,n,m',n'=-1}^1 (-1)^q \text{tr}\{[O_i, A_{n',m'}][A_{n,m}O_j^\dagger]\}J_{n,m} + \\ \sigma_{\text{gg}}^2 \sum_{n=-1}^1 (-1)^n \text{tr}\{[O_i, A_{-n,0}][A_nO_j^\dagger]\}J_{n,0} + \\ \sigma_{\text{ag}}^2 \sum_{m,n,m',n'=-1}^1 [(-1)^q \delta_{m',0} \text{tr}\{[O_i, A_{n'}][A_{n,m}O_j^\dagger]\}J_{n,m} + \\ (-1)^{q'} \delta_{m,0} \text{tr}\{[O_i, A_{n',m'}][A_nO_j^\dagger]\}J_{n,0}]$$

where the sums are subject to the constraint that $q = m' + n' = -(m + n)$. This form for the rates shows which elements are coupled to others and uniquely identifies the specific relaxation rates R_{1e} , R'_{1e} , R_{2e} , R'_{2e} , R_{1x} , and R_{2x} . The equations are robust enough to handle any size spin system, and in particular may be used for both ^{14}N or ^{15}N spin labels. The individual relaxation rate expressions can be simplified by defining coefficients, C , which are dimensionless, real numbers on the order of unity:

$$R^{ij} = \sigma_{\text{aa}}^2 \sum_{m,n=-1}^1 C_{n,m}^{ij} J_{n,m} + \sigma_{\text{gg}}^2 \sum_{n=-1}^1 C_n^{ij} J_{n,0} + \\ \sigma_{\text{ag}}^2 \sum_{m,n=-1}^1 C_{n,m}^{ij} J_{n,m} \quad (\text{A-7})$$

Where the coupling coefficients are defined as:

$$C_{n,m}^{ij} = \sum_{m',n'=-1}^1 (-1)^q \text{tr}\{[O_i, A_{n',m'}][A_{n,m}O_j^\dagger]\} \\ C_n^{ij} = (-1)^n \text{tr}\{[O_i, A_{-n,0}][A_nO_j^\dagger]\} \\ C_{n,m}^{ij} = \sum_{m',n'=-1}^1 [(-1)^q \delta_{m',0} \text{tr}\{[O_i, A_{n'}][A_{n,m}O_j^\dagger]\} + \\ (-1)^{q'} \delta_{m,0} \text{tr}\{[O_i, A_{n',m'}][A_nO_j^\dagger]\}]$$

$C_{n,m}^{ij}$, with two sub-indices, is the term that defines how the END dipolar operator produces relaxation. The coupling term with the single sub-index, C_n^{ij} , arises from the CSA operator alone, and $C_{n,m}^{ij}$ is the total cross coupling between the END and CSA Hamiltonians.

Thus far, the equations have been independent of the number of the spin operators, and the associated size of the problem. To demonstrate the utility of this theory to define the effects of the various terms, and to understand the differences between the CSA-END cross term and the END and CSA terms, we apply it to two coupled spin $1/2$ particles—the case for an ^{15}N nitroxide spin label. We first define what operators are needed for this system. There is a need for S_p and I_p —the spin operators for the two particles—and the identity operator 1. The product of these creates a total of 16 operators. If we list them in order and number them, we can discuss the relaxation processes in terms of the elements that are connected:

$$\begin{pmatrix} \langle O_1 \rangle \\ \langle O_2 \rangle \\ \langle O_3 \rangle \\ \langle O_4 \rangle \\ \langle O_5 \rangle \\ \langle O_6 \rangle \\ \langle O_7 \rangle \\ \langle O_8 \rangle \\ \langle O_9 \rangle \\ \langle O_{10} \rangle \\ \langle O_{11} \rangle \\ \langle O_{12} \rangle \\ \langle O_{13} \rangle \\ \langle O_{14} \rangle \\ \langle O_{15} \rangle \\ \langle O_{16} \rangle \end{pmatrix} = \begin{pmatrix} \langle 11 \rangle \\ \langle S_{-1}1 \rangle \\ \langle S_01 \rangle \\ \langle S_{+1}1 \rangle \\ \langle 1I_{-1} \rangle \\ \langle 2S_{-1}I_{-1} \rangle \\ \langle 2S_0I_{-1} \rangle \\ \langle 2S_{+1}I_{-1} \rangle \\ \langle 1I_0 \rangle \\ \langle 2S_{-1}I_0 \rangle \\ \langle 2S_0I_0 \rangle \\ \langle 2S_{+1}I_0 \rangle \\ \langle 1I_{+1} \rangle \\ \langle 2S_{-1}I_{+1} \rangle \\ \langle 2S_0I_{+1} \rangle \\ \langle 2S_{+1}I_{+1} \rangle \end{pmatrix}$$

END/Dipolar Relaxation. We have computed all of the elements of the C 's for the dipolar coupling—for two coupled spin $1/2$ particles there are $16 \times 16 \times 9 = 2304$ elements. Fortunately, most of them are zero. The END mechanism will self-relax each element, except the identity, $\langle O_1 \rangle$, and the END mechanism does *not* couple any single operator observables to any double operator observables. There are only eight pairs of operators that are cross coupled—couplings between $\langle S_p \rangle$ and $\langle I_p \rangle$ where $p = -1, 0$, or $+1$ —and these represent the traditional dynamic Overhauser effect cross coupling terms. There are cross couplings that parallel the traditional terms: $\langle S_p I_0 \rangle$ to $\langle S_0 I_p \rangle$ where $p = +1$ or -1 but not $p = 0$. The direct relaxation of the $p = 0$ term $\langle S_0 I_0 \rangle$ is the END contribution to the rate that has been regarded as $R_{1e} + R_{1n}$ in previous treatments.⁹ In addition, this relaxation couples $\langle S_0 I_0 \rangle$ to $\langle S_{-p} I_p \rangle$ and finally $\langle S_p I_{-p} \rangle$ to $\langle S_{-p} I_p \rangle$ for $p = +1$ or -1 . In summary: out of the 120 possible cross coupling terms, only eight are nonzero. Only the dynamic Overhauser effect cross couplings are seen, and the END by itself does not couple (or cross relax) $\langle S_p \rangle$ to $\langle S_q I_{q'} \rangle$ for any values of p , q , and q' . This result is relevant to the discussion in the main text in which it was stated that there is no cross relaxation between $\langle S_p \rangle$ and $\langle S_{-p} I_0 \rangle$ by the END mechanism alone. Moreover, the END mechanism alone does not couple $\langle S_{+1} \rangle$ to $\langle S_{-1} \rangle$.

As an example of $C_{n,m}^{ij}$ consider the coefficients that self-relax. This is the case where $i = j = 3$ and n and m have values $-1, 0$, and $+1$. Working out the products we get the coupling elements as a 3 by 3 matrix:

$$\hat{C}^{3,3} = \frac{1}{20} \begin{pmatrix} 1 & 1/2 & 1/6 \\ 0 & 0 & 0 \\ 1/6 & 1/2 & 1 \end{pmatrix}$$

The center row ($n = 0, m = -1, 0, +1$) is all zeros, ensuring that terms in the spectral density functions $J_{n,m}$ that would be independent of the electron Larmor frequency ω_0 do not contribute to the relaxation of $\langle S_0 \rangle$. It is a general observation from Abragam's treatment that the transverse components do not contain spectral densities that are independent of the spin's Larmor frequency. This result is confirmed here. There should be a similar relaxation process for the nucleus, and this is indeed the case. The relaxation of $\langle I_0 \rangle$ happens when $i = j = 9$ and $\hat{C}^{9,9} = \hat{C}^{3,3\dagger}$, which guarantees that $\langle I_0 \rangle$ spectral density functions have no terms that are independent of ω_n .

CSA Relaxation. The CSA is solely an electron operator, and therefore cannot relax the nuclear terms (observables of

the form $\langle I_q \rangle$). The CSA only relaxes the individual elements to themselves and generates no cross relaxation. In the body of the paper we stated that the direct relaxation of $\langle 2S_o I_o \rangle$ has the form $R_{1e} + R_{1n}$, where R_{1e} is the relaxation of $\langle S_o \rangle$ and R_{1n} is the relaxation of $\langle I_o \rangle$. How reasonable is it to approximate the relaxation rate of $\langle 2S_o I_o \rangle$ as the sum $R_{1e} + R_{1n}$? The observable $\langle S_o \rangle$ is element 3; $\langle I_o \rangle$ is 9. The eleventh observable element is $\langle 2S_o I_o \rangle$, and we ask, is $R_{11,11} = R_{3,3} + R_{9,9}$? This can be answered by examining the C coefficients, i.e., by comparing $C^{11,11}$ with the sum of $C^{3,3} + C^{9,9}$, the contributions of the dipolar terms.

The coefficient $C^{11,11}$ has the form

$$\frac{1}{20} \begin{pmatrix} 0 & 1/2 & 0 \\ 1/2 & 0 & 1/2 \\ 0 & 1/2 & 0 \end{pmatrix}$$

which can be compared with that of

$$C^{3,3} + C^{9,9} = \frac{1}{20} \begin{pmatrix} 1 & 1/2 & 1/6 \\ 0 & 0 & 0 \\ 1/6 & 1/2 & 1 \end{pmatrix} + \frac{1}{20} \begin{pmatrix} 1 & 0 & 1/6 \\ 1/2 & 0 & 1/2 \\ 1/6 & 0 & 1 \end{pmatrix} = \frac{1}{20} \begin{pmatrix} 2 & 1/2 & 1/3 \\ 1/2 & 0 & 1/2 \\ 1/3 & 1/2 & 2 \end{pmatrix}$$

From this we see that the elements of $C^{3,3} + C^{9,9}$ equal those of $C^{11,11}$ only for the single frequency components ($m = 0, n = +1$ or -1 , and $n = 0, m = +1$ or -1) with value $1/2$. No terms that contain either the sum or the difference of the electron and nuclear frequencies contribute to the relaxation of $\langle 2S_o I_o \rangle$. This result is a bit surprising and requires explanation. Consider the operator that represents the term in a Hamiltonian that would give rise to a spectral density term containing $(\omega_o + \omega_n)$ for element eleven. The commutator is

$$[S_+ I_+, 2S_o I_o] = 2S_+ [I_+, S_o I_o] + 2[S_+, S_o I_o] I_+ = -2\{S_+ I_+ S_o + S_+ I_o I_+\} = -2S_+ \{S_o + I_o\} I_+$$

At first glance it appears that this commutator is nonzero. However, because of its form it can only produce a nonzero result when operating on $|^{-1/2, -1/2}\rangle$, all other terms will vanish because of the raising of both the electron and nuclear indices. However, even this term vanishes because the result is $S_+ \{S_o + I_o\} I_+ |^{-1/2, -1/2}\rangle = \{-1/2 + 1/2\} |^{1/2, 1/2}\rangle = 0$. This result is particular to two coupled spin $1/2$ systems and is not generalizable to other systems.

How To Compute Spin-Spin and Spin-Lattice Relaxation Rates. We now outline how to use the above formulation to compute the relaxation rates for the different correlation times for both spin-lattice and spin-spin relaxation processes. Recall that we have only considered the CSA and the END terms for isotropic rotational Brownian motion. Equations 21 and 24 defining the relaxation rates in the main text can be written as

$$R_{\pm}^{2e} = \frac{1}{2} (R^{4,4} + R^{12,12}) \pm \text{Re} \left\{ \sqrt{\left(\frac{1}{2} (R^{4,4} - R^{12,12}) \right)^2 + \left(\frac{\bar{a}}{2} - R^{4,12} \right)^2} \right\}$$

for the two spin-spin relaxation rates and as

$$R_{\pm}^{1e} = \frac{1}{2} (R^{3,3} + R^{11,11}) \pm \sqrt{\left(\frac{1}{2} (R^{3,3} - R^{11,11}) \right)^2 + (R^{3,11})^2}$$

for the two spin-lattice relaxation rates. The individual elements are computed using:

$$R^{ij} = \sigma_{aa}^2 \sum_{m,n=-1}^1 C_{n,m}^{ij} J_{n,m} + \sigma_{gg}^2 \sum_{n=-1}^1 C_n^{ij} J_{n,o} + \sigma_{ag}^2 \sum_{m,n=-1}^1 C_{n,m}^{ij} J_{n,m}$$

We list the C coefficients as matrices for the particular couplings needed.

The elements for the spin-spin relaxation are

$$\hat{C}^{4,4} = \frac{1}{20} \begin{pmatrix} 0 & 0 & 0 \\ 1/2 & 2/3 & 1/2 \\ 1/6 & 1/2 & 1 \end{pmatrix}, \quad \hat{C}^{12,12} = \frac{1}{20} \begin{pmatrix} 0 & 0 & 0 \\ 0 & 2/3 & 0 \\ 1/6 & 1/2 & 1 \end{pmatrix}$$

and for the CSA term and the END-CSA cross term

$$\hat{C}_x^{4,4} = \hat{C}_x^{12,12} = \frac{1}{20} \begin{pmatrix} 0 \\ 8/3 \\ 2 \end{pmatrix} \quad \text{and} \quad \hat{C}_x^{4,4} = \hat{C}_x^{12,12} = 0$$

and for the other cross terms

$$\hat{C}_x^{4,12} = \hat{C}_x^{12,4} = \frac{1}{20} \begin{pmatrix} 0 & 0 & 0 \\ 0 & 8/3 & 0 \\ 0 & 2 & 0 \end{pmatrix}$$

The spin-lattice relaxation expressions follow.

For the dipolar coupling terms $C_{m,n}^{ij}$ we get

$$\hat{C}^{3,3} = \frac{1}{20} \begin{pmatrix} 1 & 1/2 & 1/6 \\ 0 & 0 & 0 \\ 1/6 & 1/2 & 1 \end{pmatrix}, \quad \hat{C}^{11,11} = \frac{1}{20} \begin{pmatrix} 0 & 1/2 & 0 \\ 1/2 & 0 & 1/2 \\ 0 & 1/2 & 0 \end{pmatrix}$$

and for the CSA terms and for the CSA-END cross term $\hat{C}_x^{3,3} = \hat{C}_x^{11,11} = 0$. The other terms are

$$\hat{C}_x^{3,11} = \hat{C}_x^{11,3} = \frac{1}{20} \begin{pmatrix} 0 & 2 & 0 \\ 0 & 0 & 0 \\ 0 & 2 & 0 \end{pmatrix}$$

Comparison of Freed's Theory and These Results. We now compare the results of the present treatment with that given by Freed et al.,³ for isotropic motion, their equations reduce to the following forms:

$$\begin{aligned} A &= \left(\frac{3}{20} \right) \left[(D_o^2 + 2D_2^2) \left(J(\omega_a) + \frac{7}{3} J(\omega_o) \right) \right] + \left(\frac{2}{5} \right) \left[(G_o^2 + 2G_2^2) \left(\frac{1}{3} J(0) + \frac{1}{4} J(\omega_o) \right) \right] \\ \frac{1}{2} B &= \left(\frac{1}{5} \right) \left[(D_o G_o + 2D_2 G_2) \left(\frac{4}{3} J(0) + J(\omega_o) \right) \right] \\ \frac{1}{4} C &= \left(\frac{1}{20} \right) \left[(D_o^2 + 2D_2^2) \left(\frac{8}{3} J(0) - J(\omega_a) - \frac{1}{3} J(\omega_o) \right) \right] \end{aligned} \quad (\text{A-8})$$

where $J(\omega) = \tau_c/[1 + (\omega\tau_c)^2]$. We note that

$$\begin{aligned}\frac{1}{4}\sigma_{AA}^2 &= (D_o^2 + 2D_2^2) \\ \sigma_{GG}^2 &= (G_o^2 + 2G_2^2) \\ \frac{1}{2}\sigma_{AG}^2 &= (D_oG_o + 2D_2G_2)\end{aligned}$$

These relations follow from the definitions given in Haas et al.^{21,22}

$$\begin{aligned}D_o &= \frac{1}{\sqrt{6}}\left[A_{zz} - \frac{1}{2}(A_{xx} + A_{yy})\right] \quad \text{and} \quad D_2 = \frac{1}{4}[A_{xx} - A_{yy}] \\ G_o &= \frac{\omega_o}{g}\sqrt{\frac{2}{3}}\left[g_{zz} - \frac{1}{2}(g_{xx} + g_{yy})\right] \quad \text{and} \\ G_2 &= \frac{\omega_o}{g}\frac{1}{2}[g_{xx} - g_{yy}]\end{aligned}$$

We also assume that $\omega_o \gg \omega_a \gg \omega_n$. Therefore, $J(\omega_o) = J_{\pm 1,n}$, $J(\omega_a) = J_{0,\pm 1}$, and $J(0) = J_{0,0}$.

Summing up the above expressions gives the results

$$\begin{aligned}\frac{1}{2}B &= R^{4,12} = R^{12,4} = \frac{\sigma_{AG}^2}{20}\left[\frac{8}{3}J_{0,0} + 2J_{1,0}\right] \\ A + \frac{1}{4}C &= \frac{1}{2}\{R^{4,4} + R^{12,12}\} = \sigma_{AA}^2\frac{1}{20}\left[\frac{2}{3}J_{0,0} + \frac{5}{3}J_{1,0} + \frac{1}{2}J_{0,1}\right] + \sigma_{GG}^2\frac{2}{5}\left[\frac{1}{3}J_{0,0} + \frac{1}{4}J_{1,0}\right]\end{aligned}$$

The line widths for the two EPR lines of an ^{15}N nitroxide are then

$$R_{\pm}^{2e} = \left(A + \frac{1}{4}C\right) \pm \frac{1}{2} \pm B \approx \frac{1}{2}\{R^{4,4} + R^{12,12}\} \pm R^{4,12}$$

The equality is obtained by neglecting the $R_{1e} - R'_{1e}$ term in the square root in eq 13A and in the main text. In actual calculations it has no impact on the two eigenvalues for the transverse components because \bar{a} is large.

Relation of $\langle 2S_oI_o \rangle$ to $\langle I_o \rangle$ and $\langle S_o \rangle$. When using the Solomon 4 level diagram to define relaxation processes, it has been assumed that the cross relaxation was just R_{1n} , which is equivalent to the assumption that the relaxation rate of $\langle 2S_oI_o \rangle$ should be $R_{1e} + R_{1n}$. This implies then that the relaxation of $\langle 2S_oI_o \rangle$ ($R^{11,11}$ in our notation) should be related to the relaxation of $\langle S_o \rangle$ ($R^{3,3}$) and the relaxation rate of $\langle I_o \rangle$ ($R^{9,9}$). If the Hamiltonian leading to relaxation is a sum of Hamiltonians, each of which depends only on either the S or the I spin, then it does follow that $R^{11,11} = R^{3,3} + R^{9,9}$. This holds if the individual Hamiltonians are independent of one another in the sense that they do not cross correlate. CSA and spin rotation fall into this class but dipolar couplings do not. To show this, we begin with eq A-2:

$$R^{j,k} = \int_{\tau=0}^{\infty} \text{tr}\{[O_j H^x(0)][H^x(\tau) O_k^\dagger]\} d\tau$$

Assume that the Hamiltonian only depends on the S spin, and

the O is the product of two normalized tensor operators for $\langle S_o \rangle$ and $\langle I_o \rangle$; the trace allows one to rearrange the order of the products, and the I spins can be removed from the commutators to give

$$R_{11+q,11+q'} = \int_{\tau=0}^{\infty} \text{tr}\{2I_o^2[\sqrt{2}S_q, H(\tau)][H(0), \sqrt{2}S_{q'}^\dagger]\} d\tau$$

The trace then can be performed on the I spins separately; for the spin $1/2$ case this sums to 1 and the effects of $\langle I_o \rangle$ drop out of the relaxation rate because the Hamiltonian is independent of $\langle I_o \rangle$:

$$R_{11+q,11+q'} = \int_{\tau=0}^{\infty} \text{tr}\{[\sqrt{2}S_q, H(\tau)][H(0), \sqrt{2}S_{q'}^\dagger]\} d\tau = R_{3+q,3+q'}$$

This result is applicable to the CSA. Therefore, it is not generally true that the two spin-lattice relaxation rates measured by pulsed-ELDOR can be regarded simply as R_{1e} and $(R_{1e} + R_{1n})$.

References and Notes

- Berliner, L. J. *Spin Labeling: Theory and Applications*; Academic Press: New York, 1976.
- Kivelson, D. *J. Chem. Phys.* **1960**, *33*, 1094–1106.
- Hwang, J. S.; Mason, R. P.; Hwang, L. P.; Freed, J. H. *J. Phys. Chem.* **1975**, *79*, 489–511.
- Robinson, B. H.; Mailer, C.; Reese, A. W. *J. Magn. Reson.* **1999**, *138*, 199–209.
- Robinson, B. H.; Mailer, C.; Reese, A. W. *J. Magn. Reson.* **1999**, *138*, 210–219.
- Lee, S.; Budil, D. E.; Freed, J. H. *J. Chem. Phys.* **1994**, *101*, 5529–5558.
- Percival, P. W.; Hyde, J. S. *J. Magn. Reson.* **1976**, *23*, 249–257.
- Atkins, P. W.; Kivelson, D. *J. Chem. Phys.* **1966**, *44*, 169.
- Robinson, B. H.; Haas, D. A.; Mailer, C. *Science* **1994**, *263*, 490–493.
- Redfield, A. G. *Phys. Rev.* **1955**, *98*, 1787–1809.
- Abraham, A. *The Principles of Nuclear Magnetism*; Oxford University Press: Oxford, U.K., 1961.
- Solomon, I. *Phys. Rev.* **1955**, *99*, 559.
- Yin, J. J.; Feix, J. B.; Hyde, J. S. *Biophys. J.* **1987**, *52*, 1031–1038.
- Freed, J. H. In *Multiple Electron Resonance Spectroscopy*; Dorio, M. M., Freed, J. H., Eds.; Plenum Press: New York, 1979; pp 73–142.
- Edmonds, A. R. *Angular Momentum in Quantum Mechanics*; Princeton University Press: Princeton, NJ, 1974.
- Carrington, A.; McLachlan, A. D. *Introduction to Magnetic Resonance with applications to chemistry and chemical physics*; Chapman and Hall: London, 1979.
- Goldman, S. A.; Bruno, G. V.; Freed, J. H. *J. Chem. Phys.* **1973**, *39*, 3071–3091.
- Hyde, J. S.; Froncisz, W.; Mottley, C. *Chem. Phys. Lett.* **1984**, *110*, 621–625.
- Dorio, M. M.; Freed, J. H. *Multiple Electron Resonance Spectroscopy*; Plenum: New York, 1979.
- Jing Long, D.; Eaton, G. R.; Eaton, S. S. *J. Magn. Reson., Ser. A* **1995**, *115*, 213–221.
- Haas, D. A.; Sugano, T.; Mailer, C.; Robinson, B. H. *J. Phys. Chem.* **1993**, *97*, 2914–2921.
- We believe that G_o and G_2 were wrongly defined in the Haas paper by a factor of 2. We think this was just a misunderstanding of the original definitions of these terms given in Freed's papers. It is necessary that these definitions be correct in order to reduce to the forms presented by Abraham.